

# Tackling the dimensions in imaging genetics with CLUB-PLS

Andre Altmann<sup>1</sup>, Ana C Lawry Aguila<sup>1</sup>, Neda Jahanshad<sup>2</sup>, Paul M Thompson<sup>2</sup>, Marco Lorenzi<sup>3</sup>

## Affiliations

1 Centre for Medical Image Computing (CMIC), Department of Medical Physics and Biomedical Engineering, University College London (UCL), London, UK

2 Imaging Genetics Center, Stevens Neuroimaging and Informatics Institute, Keck School of Medicine of USC, Marina del Rey, CA, USA

3 Université Côte d'Azur, Inria Sophia Antipolis, Epione Research Project, France

Corresponding author:

Andre Altmann

Centre for Medical Image Computing (CMIC)

Department of Medical Physics and Biomedical Engineering

University College London

90 High Holborn, 1<sup>st</sup> Floor

London WC1V 6LJ

Email: [a.altmann@ucl.ac.uk](mailto:a.altmann@ucl.ac.uk)

## **Abstract**

A major challenge in imaging genetics and similar fields is to link high-dimensional data in one domain, e.g., genetic data, to high dimensional data in a second domain, e.g., brain imaging data. The standard approach in the area are mass univariate analyses across genetic factors and imaging phenotypes. That entails executing one genome-wide association study (GWAS) for each pre-defined imaging measure. Although this approach has been tremendously successful, one shortcoming is that phenotypes must be pre-defined. Consequently, effects that are not confined to pre-selected regions of interest or that reflect larger brain-wide patterns can easily be missed. In this work we introduce a Partial Least Squares (PLS)-based framework, which we term Cluster-Bootstrap PLS (CLUB-PLS), that can work with large input dimensions in both domains as well as with large sample sizes. One key factor of the framework is to use cluster bootstrap to provide robust statistics for single input features in both domains. We applied CLUB-PLS to investigating the genetic basis of surface area and cortical thickness in a sample of 33,000 subjects from the UK Biobank. We found 107 genome-wide significant locus-phenotype pairs that are linked to 386 different genes. We found that a vast majority of these loci could be technically validated at a high rate: using classic GWAS or Genome-Wide Inferred Statistics (GWIS) we found that 85 locus-phenotype pairs exceeded the genome-wide suggestive ( $P < 1e-05$ ) threshold.

## Introduction

Imaging genetics strives to identify genetic loci that influence imaging-derived phenotypes. Thus far, the imaging genetics approach is most widely applied in the neuroscience field where the phenotypes are typically obtained from magnetic resonance imaging (MRI) scans of the human brain. One appeal of the imaging genetics approach, in contrast to classic case-control genetic analyses, is that phenotypes derived from imaging data can quantify ongoing disease processes and thus boost statistical power to identify disease relevant genetic loci. Moreover, the imaging genetics approach can be used to identify genetic influences on brain development and brain aging that are independent of disease.

Since its conception, the prevailing method in imaging genetics remains the mass univariate genome-wide association study (GWAS) approach where each imaging phenotype is tested individually against all SNPs using linear regression. Growing sample sizes and world-wide collaborative studies (Medland *et al.*, 2014) have led to a great success of this approach in identifying genetic influences on intracranial volume (Stein *et al.*, 2012), subcortical volumes (Hibar *et al.*, 2015), cortical morphology (Grasby *et al.*, 2020), and many other MRI-derived phenotypes (Elliott *et al.*, 2018). However, the application of the standard GWAS methodology has limitations. The main one being that imaging phenotypes have to be preselected and studies are therefore often based on available brain parcellations (Stein *et al.*, 2012; Medland *et al.*, 2014; Hibar *et al.*, 2015; Elliott *et al.*, 2018; Grasby *et al.*, 2020). Genetic effects that influence sub-regions or cross regional boundaries may therefore evade detection. Moreover, influences on large-scale brain organization, such as left-right asymmetry or expansion along the anterior-posterior gradient, may be missed entirely because they have not been explicitly modeled.

Numerous machine learning approaches are being investigated to overcome the limitation of mass-univariate testing in imaging genetics (Shen and Thompson, 2019). However, learning-based approaches face a major challenge due to the low explanatory power of individual single nucleotide polymorphisms (SNPs), the main genetic marker investigated in imaging genetics, on phenotypes. In recent work, Shin *et al.* (2020) first applied principal component analysis (PCA) to the imaging data and then investigated the genetic associations with the top two principal components (PCs) using a standard GWAS approach. In a related method, we previously used partial least squares (PLS) for an integrated analysis of genome-wide and vertex-wide data and identified genetic loci modulating the typical pattern of Alzheimer's brain pathology (Lorenzi *et*

*al.*, 2018), however, the memory constraints of this approach prohibits its application to large datasets such as the UK Biobank (UKB).

There exist further methods in the statistical genetics field that capture the genetic effects of single genetic variants on complex multivariate phenotypes. For instance, canonical correlation analysis (CCA)-based approaches extract the linear combination of phenotypes that explain the largest possible amount of the covariation between the SNP and all phenotypes (Ferreira and Purcell, 2009). Effectively, this test discovers whether there is an association between the SNP and any of the phenotypes. The concept has been used to investigate the genetic architecture of face and brain morphology (Claes *et al.*, 2018; Naqvi *et al.*, 2021). A further recent example is the Multivariate Omnibus Statistical Test (MOSTest) (van der Meer *et al.*, 2020), which leverages shared genetic signal between phenotypes to boost statistical power. These approaches attempt to partially alleviate the multiple-testing burden in imaging genetics application by exploiting the correlation structure of the imaging phenotypes. However, these methods treat every genetic variant independently of the rest and essentially remain standard massively univariate GWAS. Notably, the imaging genetics field has generated a range of machine learning approaches (Shen and Thompson, 2019). For instance, sparse reduced rank regression, which is a special type of multivariate multiple regression models for identifying multi-SNP and multi-phenotype associations (Vounou *et al.*, 2012). Other approaches in this area seek to integrate knowledge about gene-gene interactions and other biological priors such as molecular pathways as constrains in structured regularized machine learning approaches, e.g., (Silver *et al.*, 2012). However, despite their appeal, often the computational burden for these approaches requires pre-selection of a few thousand SNPs. Thus, rendering them ill-suited for discovery analyses.

Here we extend our previous work and introduce CLUster Bootstrap PLS (CLUB-PLS), which enables computing PLS solutions for high dimensional data as well as arbitrary large sample sizes and provides at the same time a statistical interpretation of feature weights using an efficient bootstrap approach. CLUB-PLS is applied to 33,000 participants of the UK Biobank project.

## Methods

### *Discovery*

The discovery data comprises N=38,724 subjects from UK Biobank (UKB) with available genome-wide genotyping data and T1-weighted MRI imaging data. We restricted the subjects to central European ancestry based on genetic clustering provided by UKB and successful extraction of regional surface area (66 regions) and regional cortical thickness (66 regions) based on the Desikan-Killiany (DK) atlas (Desikan *et al.*, 2006) obtained using FreeSurfer v6.0 (Dale *et al.*, 1999; Fischl *et al.*, 1999). This resulted in a set of 33,725 eligible subjects for the analysis.

The number of genotyped SNPs was 805,426. For the analysis we retained only autosomal SNPs with a minor allele frequency of at least 1% and a maximum missingness rate of 2% leading to a set of 582,538 SNPs. Following these steps, 635 subjects with a high fraction of missing SNPs were excluded, resulting in a final set of 33,070 subjects. We used the conventional additive coding for SNPs, i.e., counting the number of minor alleles. The proposed analysis approach requires a complete genetic matrix without missing values; thus we used mean imputation to fill the few missing values. Furthermore, each SNP was centered (i.e., the mean was zero).

The imaging data comprising 132 regions are subject to influences from age, sex and intra cranial volume (ICV). Thus, we regressed the effect of age (at imaging), age<sup>2</sup>, ICV, sex and the first 20 genetic principal components for population structure using linear regression. The mean of the resulting residuals was zero and, in addition, the residuals were scaled to standard deviation of 1.0.

### *Partial Least Squares*

The statistical approach for this imaging genetic analysis is based on the partial least squares (PLS) method. PLS aims to find linear projections for the two input modalities such that in the projected space they have maximal covariation. In particular, we relied on the PLS version implemented using singular value decomposition (SVD). Briefly, let  $X \in R^{N \times p1}$  be the matrix of imaging data (p1=number of imaging features),  $Y \in R^{N \times p2}$  be the matrix of genetic data (p2=number of genetic features), and  $N$  be the sample size. Then the cross-covariance matrix  $C = X^T Y$  can be decomposed using SVD:

$$C = U D V^T$$

, where the columns of  $U$  are the left singular vectors of  $C$ , the columns of  $V$  are the right singular vectors and  $D$  is a diagonal matrix of the singular values. In particular,  $U$  contains the weights for the imaging features, while  $V$  contains the weights for the genetic features such that the projections of  $U$  and  $V$  onto the data matrices  $X$  and  $Y$  maximally covary.

However, in cases where  $p_1$  and  $p_2$  are high-dimensional, the cross-covariance matrix becomes prohibitively large. Previously, we used the approach described by Worsley *et al.* (2005) based on eigenvalue decomposition that avoids the explicit computation of  $C$  to conduct an imaging genetics analysis on SNP-level and vertex-level (Lorenzi *et al.*, 2018):

$$(X^T X Y^T Y) A = A L$$

, where the columns of  $A$  contain the eigenvectors and  $L$  contains the eigenvalues, with  $D = L^{1/2}$ . Setting  $B = A(A^T Y^T Y A)^{-1/2}$ . Then, the left singular matrix  $U$  can be then computed as  $U = X(Y^T Y B L^{-1/2})$ , while the right singular matrix  $V$  can be computed as  $V = Y B$ . Thus, avoiding the need to calculate the  $p_1$  by  $p_2$  matrix  $C$ . However, this does not alleviate the computational challenges when  $N$  is large.

We recently extended this PLS approach to afford computation in a federated fashion where data are distributed across different sites (Lorenzi *et al.*, 2017). Briefly, in this federated or *meta PLS* setting each site computes a local solution to the PLS problem using only data that is available at that site, then the local solutions are shared with a central processor that computes the approximated global solution reflecting all participating samples. In this work, we employed meta PLS to scale the PLS approach to work with datasets comprising many subjects (i.e., large  $N$ ). By splitting a locally available large dataset into several (equally sized) ‘chunks’, this approach enables us to work locally with arbitrary large dataset: the PLS solution for each chunk is computed and then combined in the meta PLS fashion to obtain the approximated overall solution, similar to the group-PCA approach used in fMRI analyses (Smith *et al.*, 2014). Here, we randomly selected 33,000 subjects and split the available data into 66 chunks each comprising 500 subjects. The combination of meta PLS with the eigenvalue approach enables us to obtain PLS solutions for views with high dimensionality (large  $p_1$  and/or  $p_2$ ) as well as arbitrary large sample sizes (large  $N$ ).

### *Cluster bootstrap*

A single execution of the meta PLS algorithm using all 66 clusters results in the matrices  $U$  and  $V$ , containing weights for the imaging and genetic PLS components, respectively. However, this

single execution lacks information on the variability of these PLS weights and therefore does not provide the means to assess whether the weights are in fact substantially different from 0; thus  $p$ -values for PLS weights cannot be obtained. In previous work (Lorenzi *et al.*, 2018), we used repeated split-half cross-validation to estimate the stability selection of PLS weights and thereby their feature importance. In the absence of a sound theoretical framework to compute standard errors of the PLS weights, we propose using the bootstrap (Efron, 1992) as a wide-spread empirical method to obtain such standard error estimates. However, a straightforward application of the bootstrap would entail sampling with replacement from the entire dataset comprising 33,000 subjects and repeating the entire pipeline each time. Thus, creating a significant computational overhead. Instead, we apply the ‘cluster bootstrap’, where the sampling is not applied to the subject-level data, but to pre-defined sets or clusters. In our application, we use as clusters the 66 chunks comprising 500 subjects each. The cluster bootstrap has been shown to work with a sufficiently large number of clusters (30 or more) (Cameron *et al.*, 2008). By combining the cluster bootstrap with meta PLS we can leverage the pre-computed PLS solutions for each cluster and compute the desired standard errors for PLS weights in a computationally efficient way. We computed 500 bootstrap replications of the PLS on the entire set of 33,000 subjects to obtain means and standard deviations of PLS weights and to compute  $p$ -values based on the Wald statistic. Briefly, each of the  $k=1, \dots, K$  cluster bootstrap executions results in a left and right singular matrices  $U^*_k$  and  $V^*_k$ , respectively. (We will show the remaining derivation only for  $U$  since the same applies to  $V$ .) Next, we can estimate the average bootstrap estimate  $\bar{U}^* = \frac{1}{K} \sum_{k=1}^K U^*_k$ . Likewise, we can estimate the bootstrap standard error  $S^* = (\frac{1}{K-1} \sum_{k=1}^K (\bar{U}^* - U^*_k)^2)^{1/2}$ .

Now, for feature  $i \in \{1, \dots, p\}$  in PLS component  $c$  we get following Wald statistic:

$w_{i,c} = (U_{i,c} - \bar{U}_{i,c}^*) / S^*_{i,c}$ , which is asymptotically normally distributed if the number of clusters is large enough. Thus, using cluster bootstrap we can derive  $p$ -values for imaging features and genetic features from the PLS method. Moreover, as a benefit of using the (cluster) bootstrap there are (clusters of) subjects that have not been used for estimating the PLS model and therefore these subjects can be used to estimate the out-of-sample correlations between the imaging and genetics projections. We refer to this combination of cluster bootstrap and meta PLS as CLUB-PLS (for CLUster Bootstrap PLS).

### *Application of CLUB-PLS to the UK Biobank*

To illustrate the potential of CLUB-PLS, we computed the first ten PLS components for cortical thickness (CT) and surface area (SA) each paired with genome-wide SNP data. Within each genetic component we set the genome-wide significance threshold of  $P < 5e-08$  to identify loci of interest. Genome-wide significant loci were annotated using the SNP2GENE tool in FUMA (v1.5.5) (Watanabe *et al.*, 2017). SNPs were mapped to genes by position (within 10kb distance), eQTL (using all brain tissues available in GTEx v8 (GTEx Consortium, 2015)), and 3D chromosome interactions maps (fetal and adult cortex (Giusti-Rodríguez *et al.*, 2018), hippocampus and neural progenitor cells (Schmitt *et al.*, 2016)).

### *Validation using UK Biobank GWAS summary statistics*

We assessed how well the discovered genetic loci using CLUB-PLS can be replicated using traditional GWAS approaches. To this end we relied on results from mass univariate testing for individual regions' CT and SA measures carried out in the UK Biobank (Smith *et al.*, 2021). We used the GWIS method (Nieuwboer *et al.*, 2016) to convert the associations with individual regions to statistics for multivariate imaging patterns generated by CLUB-PLS. In brief, we used the projection weights for the imaging component  $U$  to provide the weights for the linear combination of existing summary statistics, similar to the work by Shin *et al.* (2020). We expect highly significant loci to be identified by CLUB-PLS to also exhibit a strong signal in the GWIS-based validation.



## Results

We have applied our CLUB-PLS approach to investigate the link between genetics and cortical surface area as well as cortical thickness in 33,000 subjects of the UK Biobank. The bootstrap component enabled us to compute out-of-sample correlation results between the genetic projection and the projection of the imaging data (**Table 1**). Among the first ten PLS components, correlations between surface area (SA) and genetics were higher (Pearson's  $r$  ranging from 0.084 to 0.184) than between cortical thickness (CT) and genetics (Pearson's  $r$  ranging from 0.006 to 0.118). There were 79 and 28 loci exceeding the cutoff for genome wide significance ( $P=5e-08$ ) across the top five PLS components for SA (**Table 2**) and CT (**Table 3**), respectively.

### *Genetics of cortical surface area*

**Figure 1** depicts the Manhattan plots for the first five components along with the associated brain maps. There are 18 loci exceeding the genome-wide significance threshold ( $P<5e-8$ ) for Component 1. The imaging phenotype associated with this component models overall brain surface area (as indicated by all imaging weights having the same sign; **Figure 1a**). The imaging phenotype associated with component 2 scales the surface area of the occipital lobe (**Figure 1b**) and there are 40 associated loci. Component 3 describes reduced area in the inferior parietal, the inferior and middle temporal lobes as well as the banks of the superior and temporal sulcus. At the same time the component describes an increase in area of the transverse temporal and the superior frontal lobes (**Figure 1c**). The matching genetic component yields 18 significant loci. Component 4 models reduction in the postcentral gyrus and paracentral lobule and increase frontal pole, middle temporal gyrus and pars orbitalis and was only associated with a single genome-wide significant locus (**Figure 1d**). Lastly, component 5 describes decreases in SA for superior temporal gyrus and transverse temporal gyrus and SA increases in lateral orbitofrontal cortex, pars orbitalis and medial orbitofrontal cortex. There were two genome-wide significant loci associated with this pattern (**Figure 1e**).

### *Genetics of cortical thickness*

**Figure 2** depicts the Manhattan plots for the first five components along with the associated brain maps. There are 17 loci exceeding the genome-wide significance threshold ( $P<5e-8$ ) for PLS Component 1. Like in the case of Surface Area, the imaging phenotype associated with this component models overall cortical thickness (as indicated by all imaging weights having the same sign; **Figure 2a**). The imaging phenotype associated with component 2 models brain-wide

asymmetry in cortical thickness between the right and the left hemisphere (**Figure 2b**). However, no loci reached genome-wide significance for this pattern. CT PLS component 3 models reduced cortical thickness in the insula cortex, the medial orbitofrontal cortex and the superior temporal gyrus. Conversely, CT in the precuneus as well as the superior parietal lobule are increased (**Figure 2c**). There are six independent loci significantly associated with this pattern. The CT PLS component 4 models increased CT of the superior frontal gyrus, the caudal and rostral middle frontal gyri as well as decreased CT of the lingual and the parahippocampal gyri (**Figure 2d**). There are four genome-wide significant loci associated with this pattern. Only one significant loci was associated with the pattern described by CT PLS component 5: increased cortical thickness along the cingulate and decreased cortical thickness entorhinal cortex, the parahippocampal gyrus and the temporal lobe (**Figure 2e**).

#### *Consistency of SNP-level statistics between CLUB-PLS and univariate reference methods*

We used published GWAS data together with the GWIS approach to produce GWAS summary statistics for multivariate brain phenotypes. The target phenotype was the weighted linear combination of the individual brain regions obtained from CLUB-PLS. Across the 416,000 overlapping SNPs, the Spearman rank correlation of  $-\log_{10}(\text{p-values})$  was higher for CT (0.58-0.83) than for SA (0.37-0.74). Overall, p-values by the two approaches are similar in magnitude as demonstrated by the scatterplots (**Figure 3**). The exception are the SNP associations for SA component 1, where CLUB-PLS p-values are much smaller (**Figure 3A**). To further investigate this discrepancy, we conducted a GWAS on the 33,000 UK Biobank participants with the imaging SA component 1 as the phenotype (as opposed to the GWIS approach). The linear model was adjusted for age (at imaging), age<sup>2</sup>, ICV, sex and the first 20 genetic principal components for population structure as in our CLUB-PLS analysis. Using GWAS instead of GWIS, there was a very strong correlation between CLUB-PLS p-values and GWAS based p-values (Spearman correlation of  $\rho=0.98$ ; **Figure S1**). Overall, of the 107 different locus-phenotype pairs, 61 showed a genome-wide significant p-value also in the GWIS or the GWAS (only for SA component 2) (**Table 2-3; Figure 4**). When lowering the requirement for a validation to genome-wide suggestive ( $P<1e-05$ ), then 85 locus-phenotype pairs could be validated (**Figure S2**).

## Discussion

In this work we introduced CLUB-PLS, which combines federated PLS with the cluster bootstrap technique to enable PLS computations on datasets with arbitrary large sample sizes and feature dimensions along with measures of statistical significance for the projection weights and out-of-sample correlations. As a proof-of-concept CLUB-PLS was applied to an imaging genetics task: finding genetic and imaging associations in 33,000 participants of the UK Biobank. CLUB-PLS discovered 70 loci associated with patterns of surface area and 20 loci associated with patterns of cortical thickness. With the exception for the component modeling asymmetry in cortical thickness, the out-of-sample correlation estimates from the bootstrap approach ranged from 0.075 to 0.18 which are comparable to the predictive capacity of polygenic scores in out-of-sample data reported by Grasby *et al.* (2020).

The technical validation of CLUB-PLS using GWIS and published summary statistics of regional brain measures demonstrated a good agreement between the approaches. There are various methodological differences that likely contribute to diverging results. Firstly, the used summary statistics adjusted for many covariates (see Smith *et al.* (2021) for details), while in CLUB-PLS we just adjusted for age, age<sup>2</sup>, sex, ICV and genetic principal components. Secondly, although the datasets were comparable in sample size, their composition was not identical. Thirdly, the GWIS approach only computes an approximation of effect sizes. However, despite these differences, the agreement was substantial as indicated by Spearman correlation values ranging from  $\rho=0.37-0.83$ . Moreover, conducting a GWAS with SA component 1 as the phenotype, which showed the most notable divergence between CLUB-PLS and GWIS, resulted in nearly identical statistics (Figure S1). In addition, a recent GWAS conducted for principal components of surface area by Shin *et al.* (2020) uncovered a component for general increase or decrease of SA, like our SA component 1. The most significant locus is on chr17 with a p-value  $\sim 1e-32$ , which agrees with our observation (Figure 1, top row) rather than the GWIS result we obtained.

Compared to other multivariate imaging genetics approaches, CLUB-PLS investigates all imaging features and all genetic features at the same time to extract patterns with the strongest co-variation. No other method in the field currently delivers this. The popular MOSTest approach is mass-univariate on the genetics side, and it is unclear what the multivariate imaging patterns look like that is influenced by the significant genetic loci. These patterns need to be established in post-hoc analyses. Another recent development in imaging genetics, genomic-PC (Fürtjes *et al.*, 2023), operates on summary statistics of GWAS for individual brain regions. Thus, again,

the statistics are based on mass-univariate tests. CLUB-PLS is fundamentally different since it is a method for scenarios with access to individual level genetic and imaging data.

The 107 locus-phenotype pairs were mapped to 386 genes (**Table S1**). There were various loci that influenced multiple CLUB-PLS components. For instances, locus 14:59,627,631 (rs2164950) was strongly linked to SA components 2 and 3 as well as CT component 4. This locus has been linked to five genes (*TOMM20L*, *DACT1*, *DAAM1*, *L3HYPDH*, *RTN1*) and has been previously identified in GWAS using UK Biobank data to be associated with, e.g., regional measures of surface area, cortical thickness and volume (Zhao *et al.*, 2019; Grasby *et al.*, 2020; Smith *et al.*, 2021), cortical folding (van der Meer *et al.*, 2020) and whole brain diffusion (Fan *et al.*, 2022). The locus 17:43,804,619 (Affx-13925359) was linked to component 1 of SA and CT. Interestingly, the SNP tags the common 900-kb inversion polymorphism on 17q21.31 (Stefansson *et al.*, 2005), which covers large number of genes including *MAPT*. *MAPT* encodes the microtubule-associated protein tau, which is integral to the Alzheimer's disease pathology. Mutations in *MAPT* have been linked to several neurodegenerative disorders including Alzheimer's disease (Myers *et al.*, 2005), frontotemporal dementia (Rademakers *et al.*, 2004), Parkinson's disease (Zabetian *et al.*, 2007) and dementia with lewy bodies (Colom-Cadena *et al.*, 2013). Another locus on chromosome 17 (17:2,574,821; rs12938775) was associated with SA component 1 and CT component 1, which both reflected overall increase in SA and CT, respectively. The locus was linked to *PAFAH1B1*, which is long known to be essential for brain development since loss or mutation of *PAFAH1B1* is linked to lissencephaly (Lo Nigro *et al.*, 1997), a brain malformation characterized by the absence of folds. The list of significant SNP-phenotype pairs contains many instances of loci that have been previously identified with the classic GWAS methodology (Smith *et al.*, 2021) or the MOSTest (van der Meer *et al.*, 2020) using largely the same cohort of UK Biobank participants.

The current proof-of-concept study has several limitations. Firstly, genotyped as opposed to imputed SNPs were used, likewise, the imaging dimensionality was reduced to regions of interest. However, we note that the underlying PLS approach had previously been applied to vertex level imaging data ( $p1=354,804$ ) and imputed SNPs ( $p2=1,167,126$ ) (Lorenzi *et al.*, 2017, 2018) and therefore CLUB-PLS will be able to handle these dimensions as well. The current limitation to regional imaging features enabled us to conduct a technical validation of the CLUB-PLS results, which would have been computationally impossible using vertex-level phenotypes. Secondly, this analysis represents the discovery part of the typical statistical genetic workflow, and we provided only a technical validation using published univariate GWAS results based on largely the same dataset (Smith *et al.*, 2021). Future work will require a formal

validation of the identified associations between loci and multivariate imaging patterns in an independent cohort, e.g., using the GWIS approach (Nieuwboer *et al.*, 2016) in univariate GWAS for individual brain regions such as done by Grasby *et al.* (2020). Nevertheless, we discovered a series of genetic loci that were previously described in the literature as being associated with cortical morphology. Finally, we would like to emphasize that imaging genetics is only one application field for CLUB-PLS. It is a general approach that can be used in any setting where two high-dimensional modalities are correlated. For instance, CLUB-PLS could be used instead of a sparse CCA approach in lesion to function mapping tasks (Pustina *et al.*, 2018).

## **Acknowledgements**

AA holds a Medical Research Council eMedLab Medical Bioinformatics Career Development Fellowship. This work was supported by the Medical Research Council (grant number MR/L016311/1). This research has been conducted using the UK Biobank Resource under Application Number 41127.

## References

- Cameron AC, Gelbach JB, Miller DL. Bootstrap-based improvements for inference with clustered errors. *Rev Econ Stat* 2008; 90: 414–427.
- Claes P, Roosenboom J, White JD, Swigut T, Sero D, Li J, et al. Genome-wide mapping of global-to-local genetic effects on human facial shape [Internet]. *Nat Genet* 2018 Available from: <http://www.nature.com/articles/s41588-018-0057-4>
- Colom-Cadena M, Gelpi E, Martí MJ, Charif S, Dols-Icardo O, Blesa R, et al. MAPT H1 haplotype is associated with enhanced  $\alpha$ -synuclein deposition in dementia with Lewy bodies. *Neurobiol Aging* 2013; 34: 936–942.
- Dale AM, Fischl B, Sereno MI. Cortical surface-based analysis: I. Segmentation and surface reconstruction. *Neuroimage* 1999; 9: 179–194.
- Desikan RS, Ségonne F, Fischl B, Quinn BT, Dickerson BC, Blacker D, et al. An automated labeling system for subdividing the human cerebral cortex on MRI scans into gyral based regions of interest. *Neuroimage* 2006; 31: 968–980.
- Efron B. Bootstrap methods: another look at the jackknife. In: *Breakthroughs in statistics: Methodology and distribution*. Springer; 1992. p. 569–593
- Elliott LT, Sharp K, Alfaro-Almagro F, Shi S, Miller KL, Douaud G, et al. Genome-wide association studies of brain imaging phenotypes in UK Biobank. *Nature* 2018; 562: 210–216.
- Fan CC, Loughnan R, Makowski C, Pecheva D, Chen C-H, Hagler Jr DJ, et al. Multivariate genome-wide association study on tissue-sensitive diffusion metrics highlights pathways that shape the human brain. *Nat Commun* 2022; 13: 2423.
- Ferreira MAR, Purcell SM. A multivariate test of association. *Bioinformatics* 2009; 25: 132–133.
- Fischl B, Sereno MI, Dale AM. Cortical surface-based analysis: II: inflation, flattening, and a surface-based coordinate system. *Neuroimage* 1999; 9: 195–207.
- Fürtjes AE, Arathimos R, Coleman JRI, Cole JH, Cox SR, Deary IJ, et al. General dimensions of human brain morphometry inferred from genome-wide association data. *Hum Brain Mapp* 2023
- Giusti-Rodríguez P, Lu L, Yang Y, Crowley CA, Liu X, Juric I, et al. Using three-dimensional regulatory chromatin interactions from adult and fetal cortex to interpret genetic results for psychiatric disorders and cognitive traits. *BioRxiv* 2018: 406330.
- Grasby KL, Jahanshad N, Painter JN, Colodro-Conde L, Bralten J, Hibar DP, et al. The genetic

architecture of the human cerebral cortex. *Science* (80- ) 2020; 367: eaay6690.

GTEX Consortium. Human genomics. The Genotype-Tissue Expression (GTEx) pilot analysis: multitissue gene regulation in humans. *Sci (New York, NY)* 2015; 348: 648–660.

Hibar DP, Stein JL, Renteria ME, Arias-Vasquez A, Desrivieres S, Jahanshad N, et al. Common genetic variants influence human subcortical brain structures [Internet]. *Nature* 2015 Available from: <http://www.nature.com/nature/journal/vaop/ncurrent/full/nature14101.html>

Lorenzi M, Altmann A, Gutman B, Wray S, Arber C, Hibar DP, et al. Susceptibility of brain atrophy to TRIB3 in Alzheimer's disease, evidence from functional prioritization in imaging genetics. *Proc Natl Acad Sci U S A* 2018; 115: 3162–3167.

Lorenzi M, Gutman B, Thompson P, Alexander DC, Ourselin S, Altmann A. Secure multivariate large-scale multi-centric analysis through on-line learning: an imaging genetics case study [Internet]. [discovery.ucl.ac.uk](http://discovery.ucl.ac.uk/1531135/) 2017 Available from: <http://discovery.ucl.ac.uk/1531135/>

Medland SE, Jahanshad N, Neale BM, Thompson PM. Whole-genome analyses of whole-brain data: working within an expanded search space. *Nat Neurosci* 2014; 17: 791–800.

van der Meer D, Frei O, Kaufmann T, Shadrin AA, Devor A, Smeland OB, et al. Understanding the genetic determinants of the brain with MOSTest. *Nat Commun* 2020; 11: 3512.

Myers AJ, Kaleem M, Marlowe L, Pittman AM, Lees AJ, Fung HC, et al. The H1c haplotype at the MAPT locus is associated with Alzheimer's disease. *Hum Mol Genet* 2005; 14: 2399–2404.

Naqvi S, Sleyp Y, Hoskens H, Indencleef K, Spence JP, Bruffaerts R, et al. Shared heritability of human face and brain shape. *Nat Genet* 2021; 53: 830–839.

Nieuwboer HA, Pool R, Dolan C V, Boomsma DI, Nivard MG. GWIS: genome-wide inferred statistics for functions of multiple phenotypes. *Am J Hum Genet* 2016; 99: 917–927.

Lo Nigro C, Chong SS, Smith ACM, Dobyns WB, Carrozzo R, Ledbetter DH. Point mutations and an intragenic deletion in LIS1, the lissencephaly causative gene in isolated lissencephaly sequence and Miller-Dieker syndrome. *Hum Mol Genet* 1997; 6: 157–164.

Pustina D, Avants B, Faseyitan OK, Medaglia JD, Coslett HB. Improved accuracy of lesion to symptom mapping with multivariate sparse canonical correlations. *Neuropsychologia* 2018; 115: 154–166.

Rademakers R, Cruts M, Van Broeckhoven C. The role of tau (MAPT) in frontotemporal dementia and related tauopathies. *Hum Mutat* 2004; 24: 277–295.



Schmitt AD, Hu M, Jung I, Xu Z, Qiu Y, Tan CL, et al. A Compendium of Chromatin Contact Maps Reveals Spatially Active Regions in the Human Genome. *Cell Rep* 2016; 17: 2042–2059.

Shen L, Thompson PM. Brain imaging genomics: integrated analysis and machine learning. *Proc IEEE* 2019; 108: 125–162.

Shin J, Ma S, Hofer E, Patel Y, Vosberg DE, Tilley S, et al. Global and regional development of the human cerebral cortex: molecular architecture and occupational aptitudes. *Cereb Cortex* 2020; 30: 4121–4139.

Silver M, Montana G, Initiative ADN. Fast identification of biological pathways associated with a quantitative trait using group lasso with overlaps. *Stat Appl Genet Mol Biol* 2012; 11: Article 7.

Smith SM, Douaud G, Chen W, Hanayik T, Alfaro-Almagro F, Sharp K, et al. An expanded set of genome-wide association studies of brain imaging phenotypes in UK Biobank. *Nat Neurosci* 2021; 24: 737–745.

Smith SM, Hyvärinen A, Varoquaux G, Miller KL, Beckmann CF. Group-PCA for very large fMRI datasets. *Neuroimage* 2014; 101: 738–749.

Stefansson H, Helgason A, Thorleifsson G, Steinthorsdottir V, Masson G, Barnard J, et al. A common inversion under selection in Europeans. *Nat Genet* 2005; 37: 129–137.

Stein JL, Medland SE, Vasquez AA, Hibar DP, Senstad RE, Winkler AM, et al. Identification of common variants associated with human hippocampal and intracranial volumes. *Nat Genet* 2012; 44: 552–561.

Vounou M, Janousova E, Wolz R, Stein JL, Thompson PM, Rueckert D, et al. Sparse reduced-rank regression detects genetic associations with voxel-wise longitudinal phenotypes in Alzheimer's disease. *Neuroimage* 2012; 60: 700–716.

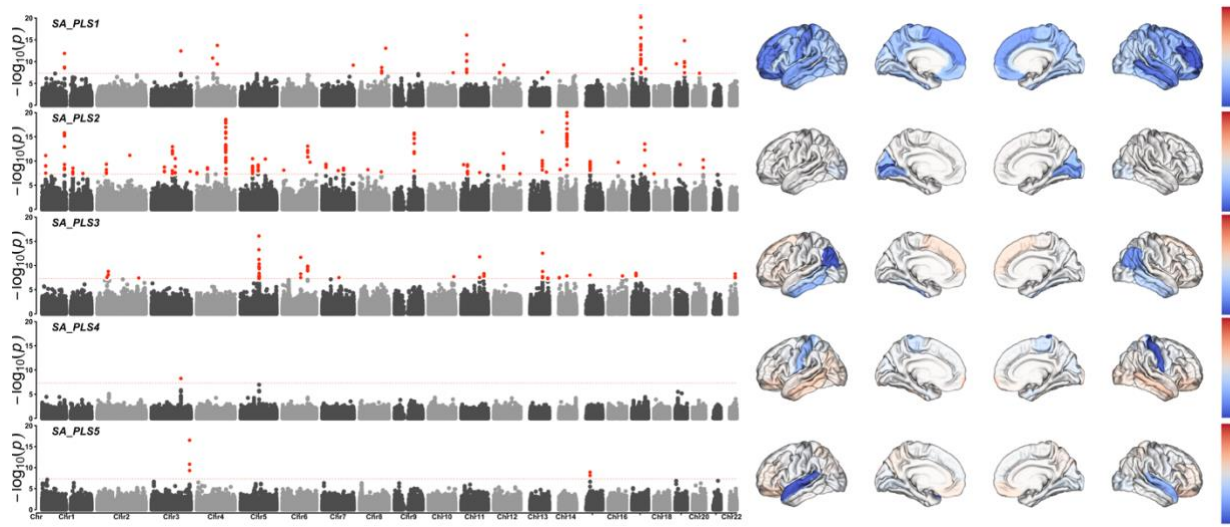
Watanabe K, Taskesen E, van Bochoven A, Posthuma D. Functional mapping and annotation of genetic associations with FUMA. *Nat Commun* 2017; 8: 1826.

Worsley KJ, Chen J-I, Lerch J, Evans AC. Comparing functional connectivity via thresholding correlations and singular value decomposition. *Philos Trans R Soc London Ser B, Biol Sci* 2005; 360: 913–920.

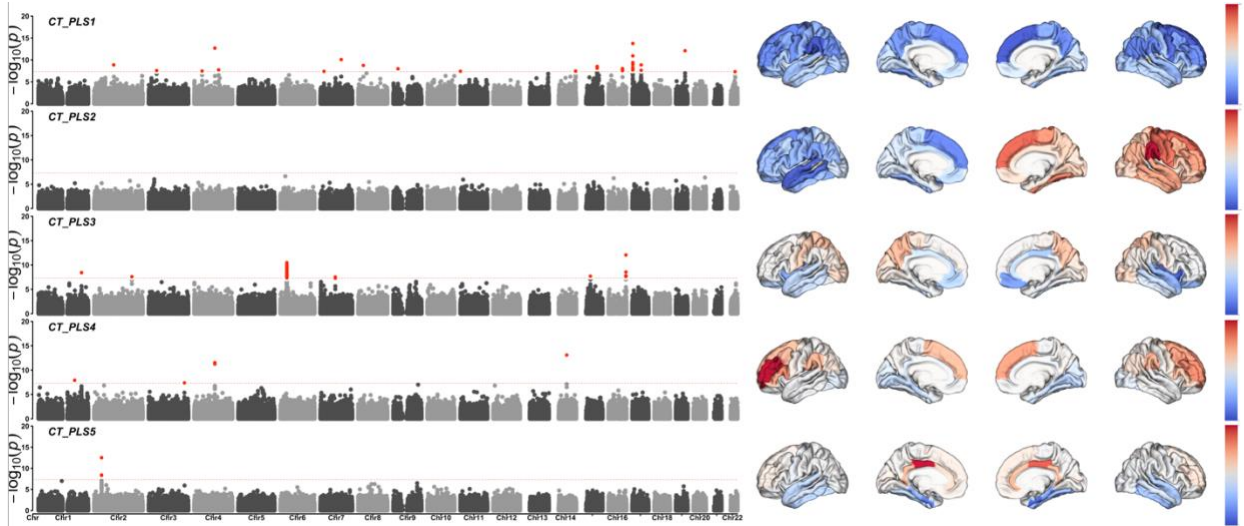
Zabetian CP, Hutter CM, Factor SA, Nutt JG, Higgins DS, Griffith A, et al. Association analysis of MAPT H1 haplotype and subhaplotypes in Parkinson's disease. *Ann Neurol* 2007; 62: 137–144.

Zhao B, Luo T, Li T, Li Y, Zhang J, Shan Y, et al. Genome-wide association analysis of 19,629 individuals identifies variants influencing regional brain volumes and refines their genetic co-architecture with cognitive and mental health traits. *Nat Genet* 2019; 51: 1637–1644.

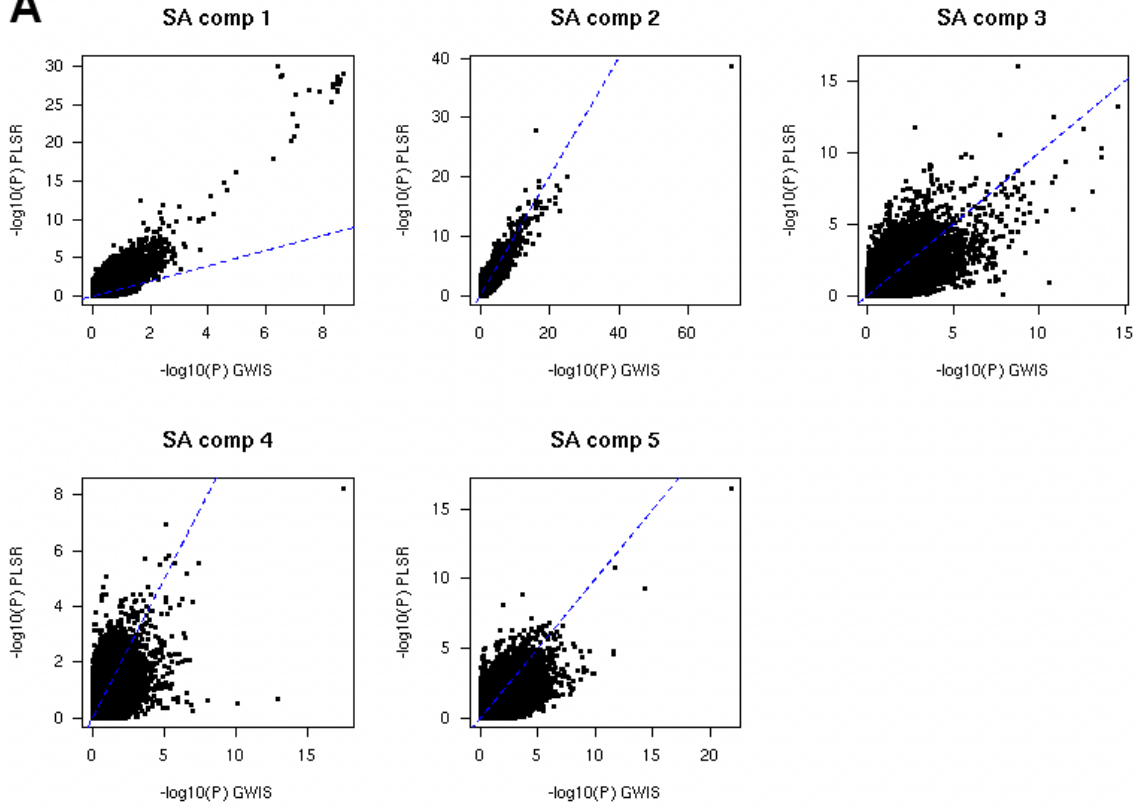
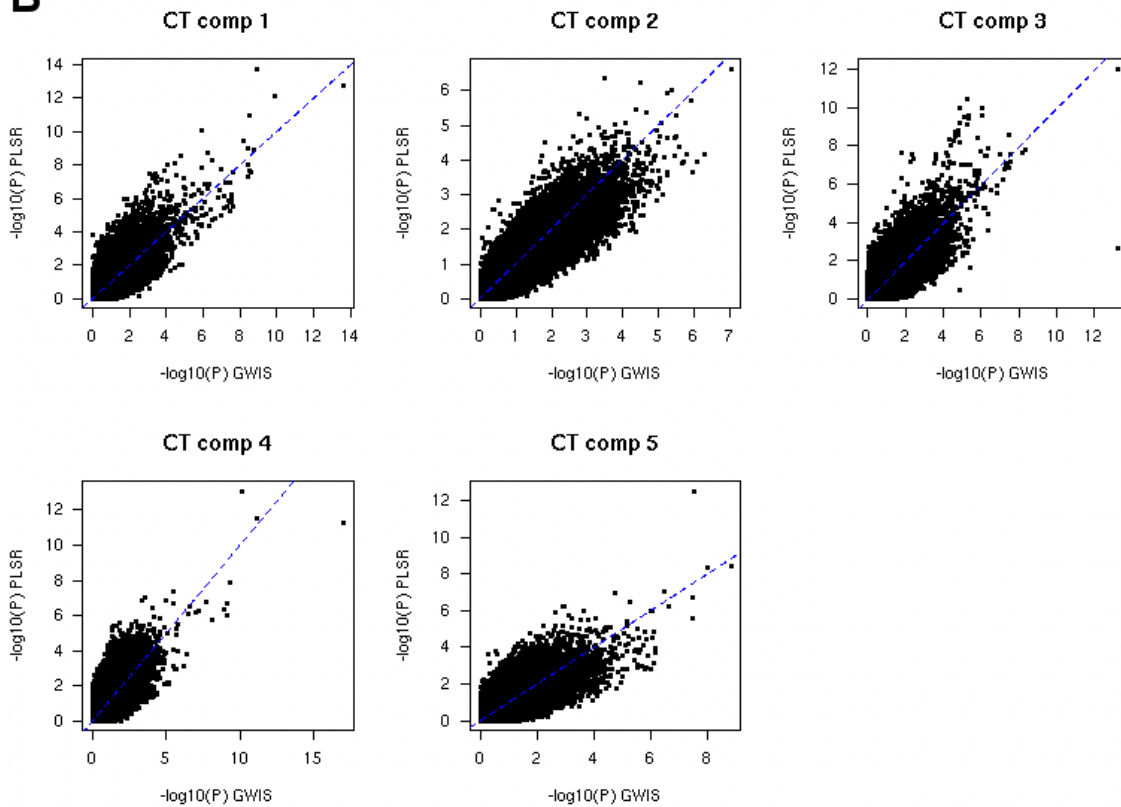
## Figures



**Figure 1: Matched genetic and imaging associations for Surface Area.** The left part of the plot shows the genetic associations extracted by CLUB-PLS for the imaging phenotype depicted in the right part. Each row corresponds to one CLUB-PLS component. Genetic associations are shown in the form of Manhattan plots with SNPs ordered by chromosomes and positions on the x-axis and the  $-\log_{10}(p)$  on the y-axis. SNPs passing the threshold for genome-wide significance are highlighted in red. The imaging components is colored based on the Wald statistic multiplied by the direction of the effect, with cold and warm colors indicating decreases and increases in SA, respectively.



**Figure 2: Matched genetic and imaging associations for Cortical Thickness.** The left part of the plot shows the genetic associations extracted by CLUB-PLS for the imaging phenotype depicted in the right part. Each row corresponds to one CLUB-PLS component. Genetic associations are shown in the form of Manhattan plots with SNPs ordered by chromosomes and positions on the x-axis and the  $-\log_{10}(p\text{-value})$  on the y-axis. SNPs passing the threshold for genome-wide significance are highlighted in red. The imaging components is colored based on the Wald statistic multiplied by the direction of the effect, with cold and warm colors indicating decreases and increases in CT, respectively.

**A****B**

**Figure 3: Correlation between CLUB-PLS and GWIS statistics for SNPs.** The scatter plots depict the  $-\log_{10}(\text{p-values})$  for GWIS (x-axis) and CLUB-PLS (y-axis) for 416,000 SNPs. The blue dashed line indicates the identity (i.e., the same p-value by both approaches). **(A)** Scatter plots for Surface Area; the Spearman correlation between these two approaches is  $\rho=0.60$ ,  $0.74$ ,  $0.48$ ,  $0.37$ , and  $0.49$ , for components 1-5, respectively. **(B)** Scatter plots for Cortical Thickness; the Spearman correlation between these two approaches is  $\rho=0.58$ ,  $0.83$ ,  $0.61$ ,  $0.58$ , and  $0.61$ , for components 1-5, respectively.

SNP validation

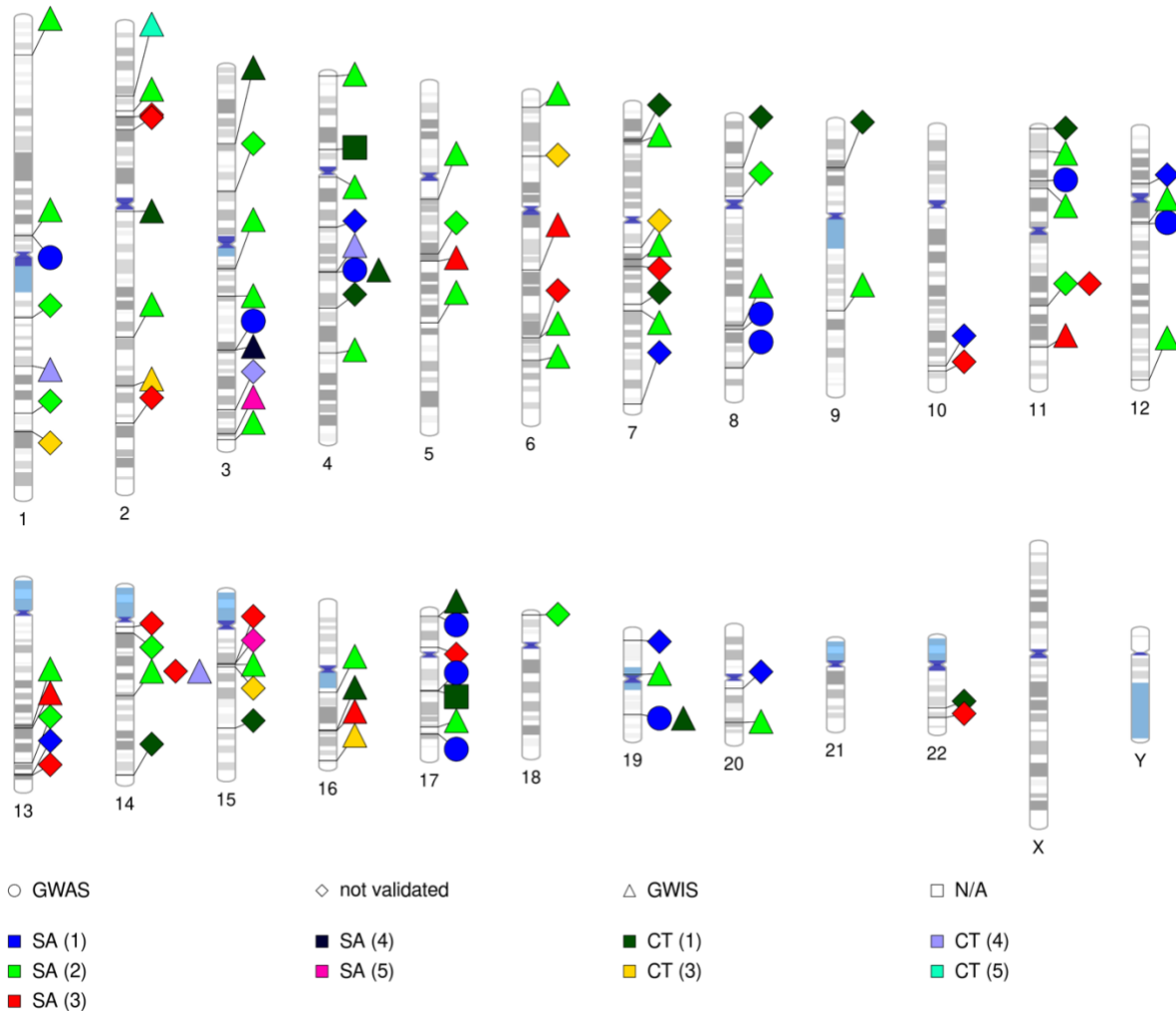


**Figure 4. Technical validation of significant hits identified by CLUB-PLS.** This ideogram depicts the loci of genome-wide significant loci identified with CLUB-PLS. Different colors indicate the different PLS components (SA=Surface Area; CT=Cortical Thickness). The symbols indicate whether the SNP-phenotype combination was validated via GWAS (circle), GWIS (triangle), missing (square) or did not reach the genome-wide significance threshold (diamond). Of the 107 individual SNP-phenotype associations, 61 also exceeded the genome-wide significance threshold ( $P < 5e-8$ ) using the GWAS or GWIS approach and two SNPs were not available in the summary statistics. The remaining 44 SNPs did not pass the genome-wide threshold.

## Tables

**Table 1: Average out of sample correlations between latent genetics and imaging components from PLS.**

Component	Cortical Thickness		Surface Area	
	correlation	p-value	correlation	p-value
<b>PLS 1</b>	0.099	1.18e-72	0.171	5.76e-215
<b>PLS 2</b>	0.006	0.28	0.184	3.83e-249
<b>PLS 3</b>	0.090	2.57e-60	0.140	4.56e-144
<b>PLS 4</b>	0.088	9.81e-58	0.116	3.20e-99
<b>PLS 5</b>	0.083	1.54e-51	0.109	9.16e-88
<b>PLS 6</b>	0.118	1.25e-102	0.122	1.27e-109
<b>PLS 7</b>	0.101	1.47e-75	0.104	5.02e-80
<b>PLS 8</b>	0.105	1.52e-81	0.102	4.93e-77
<b>PLS 9</b>	0.085	5.67e-54	0.084	9.51e-53
<b>PLS 10</b>	0.075	2.22e-42	0.087	1.82e-56

Pearson's correlation coefficient based on the average of 500 bootstrap replicates.



**Table 2. Genome-wide significant loci for the Surface Area components 1-5.**

Chrom	Position	A1	A2	SNP	BETA	SE	P	Validation P
<i>Component 1</i>								
1	113190807	C	A	rs17030613	0.00615	0.00086702	1.31E-12	2.65E-08
3	147054867	C	T	rs10513309	0.00689816	0.00094918	3.66E-13	3.51E-09
4	79832706	G	C	rs12507099	-0.0042969	0.00063724	1.55E-11	7.72E-08
4	103188709	T	C	rs13107325	-0.0055074	0.00071912	1.88E-14	8.74E-15
7	155778152	A	G	rs75745313	0.00363779	0.00058863	6.41E-10	7.70E-08
8	110603219	C	G	rs17450520	-0.005264	0.00088009	2.21E-09	2.50E-08
8	130645692	G	A	rs55705857	0.00482797	0.00064695	8.48E-14	4.96E-14
10	123996970	A	G	rs61753077	0.00271167	0.00049217	3.60E-08	2.83E-06
11	27353309	G	A	rs10835163	-0.0071583	0.00128152	2.33E-08	1.01E-09
12	28412415	TC	T	rs141906323	-0.0060594	0.00109696	3.32E-08	3.95E-07
12	49379537	T	G	rs118115924	-0.0019387	0.00031249	5.50E-10	2.80E-11
13	107095811	C	T	rs16968624	-0.0031232	0.00056247	2.81E-08	1.31E-05
17	2574821	G	A	rs12938775	0.00844408	0.00144155	4.69E-09	6.45E-10
17	43804619	T	C	Affx-13925359	0.01381989	0.00121225	4.17E-30	7.72E-33
17	68090207	T	C	rs11867479	0.00793058	0.00134683	3.90E-09	3.40E-09
19	5037351	A	G	rs263057	-0.0039072	0.00062079	3.10E-10	2.83E-06
19	46118127	T	C	rs3816046	-0.0128144	0.001254	1.63E-24	1.06E-22
20	33565169	T	C	rs6120778	0.00699092	0.00127968	4.68E-08	1.61E-07
<i>Component 2</i>								
1	18976489	C	T	rs9439714	0.00899863	0.00131447	7.60E-12	1.52E-12
1	113083439	T	C	rs10745330	0.01212021	0.00146881	1.56E-16	7.42E-18
1	155735012	C	T	rs2297775	-0.006725	0.00113394	3.02E-09	1.07E-06
1	205773461	C	T	rs708729	0.00496063	0.00090284	3.92E-08	9.32E-06
2	45170153	A	G	rs4953152	-0.0082434	0.00132278	4.61E-10	1.79E-09
2	162891075	T	C	rs2160927	0.00777548	0.00113332	6.85E-12	1.57E-11
3	64546459	T	C	rs7615657	0.00765415	0.00127311	1.83E-09	7.89E-08
3	104735446	G	A	rs28421781	0.00726027	0.0009779	1.13E-13	2.27E-12
3	118959210	T	C	rs13065867	0.00672893	0.00101343	3.14E-11	5.91E-11
3	193810750	T	C	rs7642977	-0.0069964	0.00123204	1.36E-08	1.31E-09
4	1003788	G	C	rs4569707	-0.008193	0.00147727	2.92E-08	1.12E-08
4	53727952	G	T	rs76856111	-0.0058806	0.00098692	2.55E-09	7.97E-10
4	145275039	A	G	rs6537279	-0.0100992	0.00090919	1.15E-28	1.18E-16
5	60088250	C	T	rs6873181	-0.009681	0.00146112	3.46E-11	4.54E-15
5	88354675	C	T	rs10037512	0.0071891	0.00116495	6.78E-10	7.02E-06
5	124266790	T	G	rs73302776	-0.0060895	0.00092196	3.98E-11	1.48E-14

6	7118990	A	G	rs11755724	0.00814659	0.00141186	7.92E-09	6.32E-11
6	127000881	G	A	rs74580701	0.00426351	0.00057155	8.68E-14	2.31E-15
6	138872645	T	C	rs4481452	0.00837295	0.00131309	1.81E-10	6.05E-13
7	18868031	T	C	rs17349860	-0.0085778	0.00137671	4.65E-10	4.47E-14
7	80461728	C	A	rs10251375	0.00719593	0.0012536	9.46E-09	6.24E-10
7	107283711	A	G	rs2701678	-0.0063404	0.00107016	3.13E-09	5.34E-09
8	41201081	C	A	rs13254935	0.00446019	0.0007675	6.20E-09	1.27E-07
8	108287597	A	G	rs10090742	-0.006731	0.00119371	1.71E-08	1.17E-08
9	98231908	A	G	rs28702657	0.00951485	0.00115541	1.80E-16	8.89E-15
11	12072099	G	A	rs12417334	0.00840954	0.00135698	5.75E-10	2.39E-10
11	31547227	G	T	rs502794	0.00802441	0.00129591	5.94E-10	2.10E-11
11	92453759	T	C	rs1791571	0.00693345	0.00124413	2.50E-08	5.96E-08
12	48398080	T	A	rs3803183	0.00707364	0.00101302	2.90E-12	4.16E-12
12	130578130	G	A	rs7295050	-0.0069504	0.00126885	4.31E-08	2.87E-08
13	80170160	G	A	rs2783130	-0.0134377	0.00162031	1.10E-16	9.20E-21
13	100723564	C	A	rs2151943	-0.0034033	0.00060652	2.01E-08	2.56E-06
14	25167511	A	G	rs12879771	0.00621355	0.00106756	5.87E-09	3.80E-05
14	59627631	A	G	rs2164950	0.01583882	0.00120491	1.81E-39	4.77E-73
15	39989140	A	G	rs8028503	0.00591819	0.00092046	1.28E-10	2.48E-10
16	49542037	A	G	rs12926543	0.00825526	0.00129573	1.88E-10	1.74E-12
17	63914750	G	A	rs1420791	0.00476567	0.0006273	3.03E-14	3.37E-13
18	322109	G	A	rs7236292	0.00740222	0.00135271	4.45E-08	3.51E-06
19	24021327	A	G	rs2194275	0.00579419	0.00093381	5.47E-10	1.43E-08
20	52447303	A	G	rs6022786	-0.0087427	0.00133519	5.84E-11	1.75E-17
<i>Component 3</i>								
2	48292697	T	C	rs28460586	-0.0055599	0.00100211	2.89E-08	7.54E-05
2	54858511	T	C	rs1052788	0.00621553	0.00103214	1.72E-09	0.00048741
2	207717431	C	T	rs6737069	-0.0058183	0.00105754	3.76E-08	0.0003221
5	92187932	T	C	rs17669337	-0.0120169	0.00144238	8.00E-17	1.70E-09
6	92002569	C	A	rs9345124	-0.0084063	0.00119601	2.09E-12	2.55E-13
6	126966308	C	T	rs4549631	0.00967394	0.00150717	1.38E-10	1.96E-06
7	84010609	C	T	rs34822336	0.00453894	0.00082104	3.23E-08	5.71E-05
10	126859029	A	G	rs2681919	0.00741684	0.00132318	2.08E-08	2.81E-05
11	92453759	T	C	rs1791571	0.00968131	0.00137057	1.62E-12	0.0016966
11	114186645	C	T	rs10891647	-0.0052956	0.00090529	4.93E-09	6.61E-09
13	81428951	T	C	rs7332768	0.00714369	0.00097907	2.96E-13	1.49E-11
13	107642591	C	T	rs1333186	-0.0066525	0.00121199	4.04E-08	1.82E-05
14	21578007	A	G	rs36100359	0.0045889	0.00082902	3.11E-08	0.00313837
14	59627631	A	G	rs2164950	-0.0062292	0.0011002	1.50E-08	0.0001521

15	39366899	A	C	rs4924334	0.00840011	0.00146348	9.48E-09	0.00641049
16	70661986	C	T	rs4985412	-0.0078275	0.00138118	1.45E-08	1.63E-08
17	19812541	C	T	rs203462	-0.0070801	0.00120314	3.99E-09	0.00017866
22	43824618	T	G	rs7290966	-0.0074383	0.00127534	5.46E-09	4.48E-07
<i>Component 4</i>								
3	147175324	C	T	rs12630408	0.00915116	0.00156986	5.57E-09	3.22E-18
<i>Component 5</i>								
3	190654424	C	T	rs13089287	0.01345512	0.00159297	3.00E-17	1.77E-22
15	39619456	A	C	rs8032326	-0.0070101	0.00115448	1.26E-09	0.00021828

Chrom = Chromosome; Position = base pair position on hg19; A1 = affect allele; A2 = reference allele; BETA = effect size computed by CLUB-PLS; SE = standard error; P = CLUB-PLS p-value; Validation P = GWAS (for component 1) or GWIS p-value

**Table 3: Genome-wide significant loci for the Cortical Thickness components 1-5.**

Chrom	Position	A1	A2	SNP	BETA	SE	P	Validation P
<i>Component 1</i>								
2	97668945	T	C	rs78783493	0.00515147	0.00084991	1.35E-09	1.71E-09
3	39523003	T	C	rs1768208	0.00620018	0.00111445	2.64E-08	2.67E-08
4	39302247	C	T	rs12500277	0.00237978	0.00043077	3.31E-08	N/A
4	103188709	T	C	rs13107325	0.00587969	0.00079968	1.94E-13	2.52E-14
4	121707714	T	C	rs12507922	-0.0081138	0.00144149	1.82E-08	1.11E-07
7	18008582	G	A	rs34058374	-0.0070037	0.00127528	3.98E-08	2.78E-05
7	103733264	A	G	rs10276148	0.0083364	0.00128321	8.22E-11	1.35E-06
8	26137132	A	C	rs73215685	-0.0030736	0.00051054	1.74E-09	6.39E-07
9	23529626	C	A	rs156396	-0.0064789	0.00113151	1.03E-08	9.52E-05
11	305619	T	C	rs6421984	0.00558426	0.00101466	3.72E-08	0.00046413
14	103834316	A	G	rs2403171	0.00553514	0.0010022	3.33E-08	0.00080329
15	75136261	C	G	rs6938	-0.0069693	0.00117609	3.11E-09	1.81E-05
16	70148508	A	G	rs4985397	0.00828962	0.00144345	9.31E-09	3.75E-09
17	2546340	T	C	rs74252325	-0.0080062	0.00104407	1.74E-14	1.23E-09
17	44109474	A	G	Affx-13930388	0.00814595	0.00134359	1.34E-09	N/A
19	46118127	T	C	rs3816046	0.00921296	0.00128614	7.88E-13	1.28E-10
22	38491765	T	G	rs6000996	-0.0052419	0.00095999	4.75E-08	0.00036129
<i>Component 3</i>								
1	215379943	A	G	rs2027320	0.00709248	0.00120244	3.67E-09	1.49E-06
2	188186079	A	G	rs840584	-0.007546	0.00135485	2.55E-08	2.63E-08
6	32578970	C	T	rs502771	-0.0057444	0.00086634	3.34E-11	5.98E-06
7	74094721	G	T	rs13227433	0.0057065	0.00102927	2.95E-08	0.00433
15	41427864	T	C	rs561821	0.00731508	0.00130264	1.96E-08	1.13E-06
16	87226206	T	C	rs9933149	-0.0108802	0.00152189	8.73E-13	6.21E-14
<i>Component 4</i>								
1	180962282	A	G	rs1411478	-0.0072324	0.00126922	1.21E-08	4.50E-10
3	178072001	A	G	rs2583481	0.00733272	0.00133712	4.16E-08	3.28E-06
4	102926923	A	G	rs34592089	0.00443904	0.00063599	2.96E-12	7.99E-12
14	59627631	A	G	rs2164950	0.00595363	0.00079703	8.03E-14	7.13E-11
<i>Component 5</i>								
2	37232014	A	G	rs2247935	0.00808785	0.00110935	3.09E-13	3.10E-08

Chrom = Chromosome; Position = base pair position on hg19; A1 = affect allele; A2 = reference allele; BETA = effect size computed by CLUB-PLS; SE = standard error; P = CLUB-PLS p-value; Validation P = GWIS p-value

## Supplementary Material

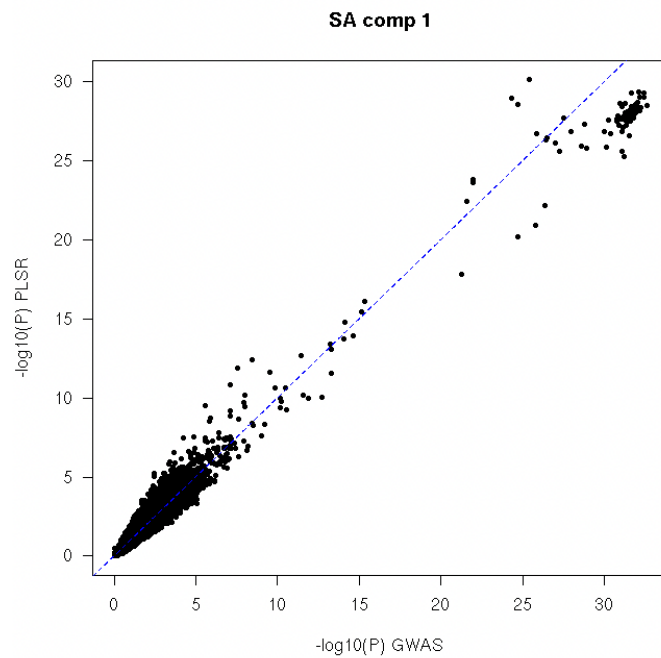


**Figure S1: Correlation between CLUB-PLS and GWAS statistics for SNPs.** The scatter plots depict the  $-\log_{10}(\text{p-values})$  for GWAS (x-axis) and CLUB-PLS (y-axis) for SA component 1. The blue dashed line indicates the identity (i.e., the same p-value by both approaches). The Spearman correlation was  $\rho=0.98$ .

SNP validation

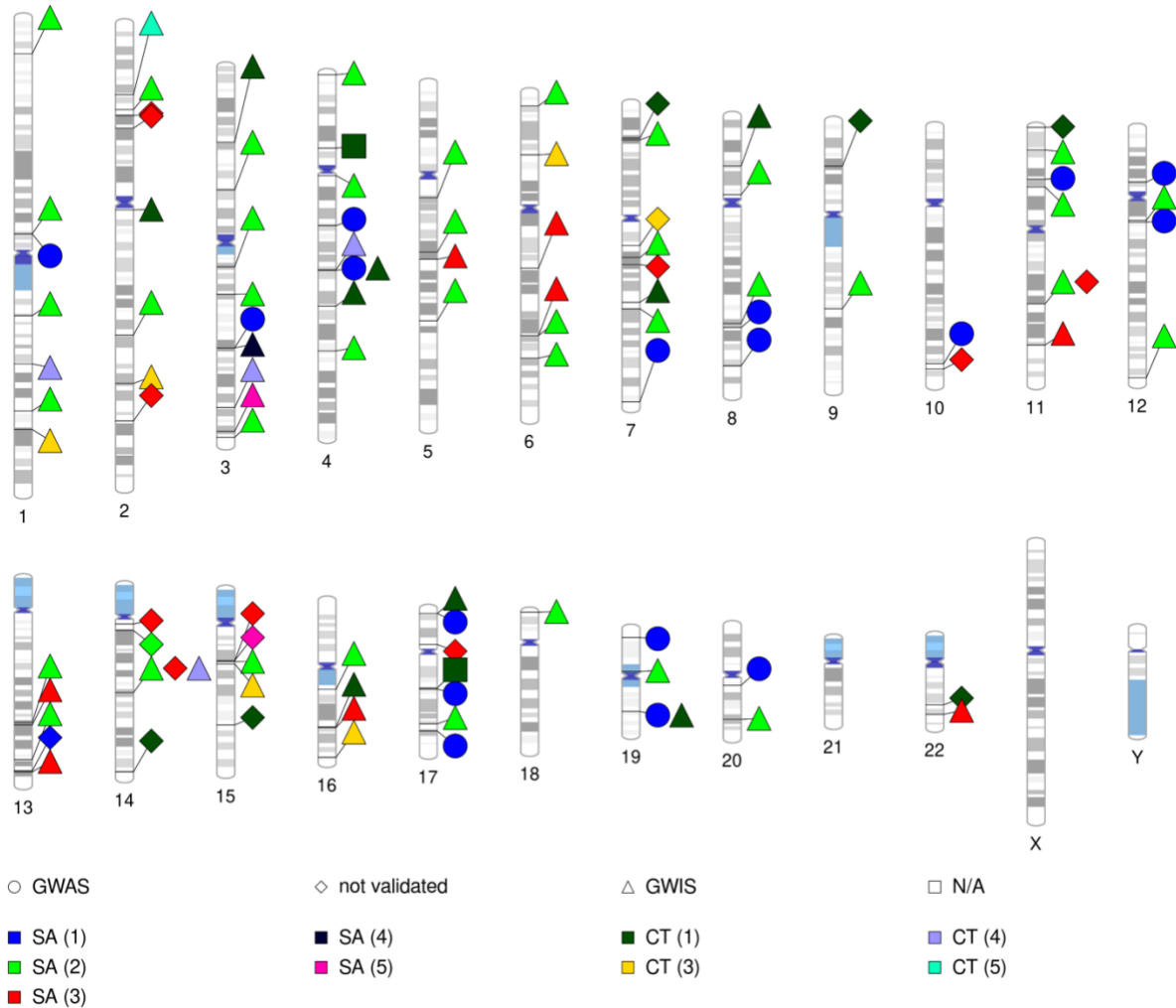


**Figure S2: Technical validation of significant hits identified by CLUB-PLS.** This ideogram depicts the loci of genome-wide significant loci identified with CLUB-PLS. Different colors indicate the different PLS components (SA=Surface Area; CT=Cortical Thickness). The symbols indicate whether the SNP-phenotype combination was validated via GWAS (circle), GWIS (triangle), missing (square) or did not reach the genome-wide suggestive threshold ( $P < 1e-5$ ; diamond). Of the 107 individual SNP-phenotype associations, 85 also exceeded the genome-wide suggestive threshold ( $P < 1e-5$ ) using the GWAS or GWIS approach and two SNPs were not available in the summary statistics. The remaining 20 SNPs did not pass the genome-wide suggestive threshold.

**Table S1: Mapped genes.** Based on the SNP2GENE function in FUMA using positional mapping (within 10kb), eQTL in GTEx Brain Tissues as well as 3D chromatin interaction maps. (File: Table\_S1.pdf).

ensg	symbol	chr	start	end	entrezID	HUGO	eqtIMapminQ	eqtI Direction	ciMap	GenomicLocus
ENSG00000009709	PAX7	1	18957500	19075360	5081	PAX7	NA	NA	Yes	1
ENSG00000143110	C1orf162	1	112016414	112021134	128346	C1orf162	NA	NA	Yes	2
ENSG00000143079	CTTNBP2NL	1	112938803	113006078	55917	CTTNBP2NL	NA	NA	Yes	2
ENSG00000134245	WNT2B	1	113009163	113072787	7482	WNT2B	1.90E-14	-	Yes	2
ENSG00000007341	ST7L	1	113066140	113163447	54879	ST7L	7.65E-09	+	Yes	2
ENSG00000116489	CAPZA1	1	113161795	113214241	829	CAPZA1	9.78E-05	+	Yes	2
ENSG00000155363	MOV10	1	113215763	113243368	4343	MOV10	NA	NA	Yes	2
ENSG00000155366	RHOC	1	113243728	113250056	389	RHOC	NA	NA	Yes	2
ENSG00000271810	RP11-426L16.10	1	113245236	113254055	NA	NA	NA	NA	No	2
ENSG00000184599	FAM19A3	1	113263041	113269857	284467	FAM19A3	NA	NA	Yes	2
ENSG00000155380	SLC16A1	1	113454469	113499635	6566	SLC16A1	NA	NA	Yes	2
ENSG00000081026	MAGI3	1	113933371	114228545	260425	MAGI3	NA	NA	Yes	2
ENSG00000134262	AP4B1	1	114437370	114447823	10717	AP4B1	NA	NA	Yes	2
ENSG00000118655	DCLRE1B	1	114447763	114456708	64858	DCLRE1B	NA	NA	Yes	2
ENSG00000163349	HIPK1	1	114471814	114520426	204851	HIPK1	NA	NA	Yes	2
ENSG00000197323	TRIM33	1	114935399	115053781	51592	TRIM33	NA	NA	Yes	2
ENSG00000163344	PMVK	1	154897210	154909467	10654	PMVK	3.03E-09	NA	No	3
ENSG00000163348	PYGO2	1	154929502	154936329	90780	PYGO2	0.00635244	NA	No	3
ENSG00000160688	FLAD1	1	154955814	154965587	80308	FLAD1	NA	NA	Yes	3
ENSG00000143537	ADAM15	1	155023042	155035252	8751	ADAM15	2.53E-06	+	No	3
ENSG00000169242	EFNA1	1	155099936	155107333	1942	EFNA1	NA	NA	Yes	3
ENSG00000169241	SLC50A1	1	155107820	155111329	55974	SLC50A1	NA	NA	Yes	3
ENSG00000179085	DPM3	1	155112367	155113071	54344	DPM3	NA	NA	Yes	3
ENSG00000273088	RP11-201K10.3	1	155141885	155159748	NA	NA	NA	NA	Yes	3
ENSG00000169231	THBS3	1	155165379	155178842	7059	THBS3	2.36E-13	NA	Yes	3
ENSG00000173171	MTX1	1	155178490	155183615	4580	MTX1	NA	NA	Yes	3



ENSG00000177628	GBA	1	155204243	155214490	2629	GBA	NA	NA	Yes	3
ENSG00000160767	FAM189B	1	155216996	155225274	10712	FAM189B	NA	NA	No	3
ENSG00000116521	SCAMP3	1	155225770	155232221	10067	SCAMP3	NA	NA	Yes	3
ENSG00000176444	CLK2	1	155232659	155248282	1196	CLK2	NA	NA	Yes	3
ENSG00000143630	HCN3	1	155247374	155259639	57657	HCN3	0.0024497	NA	Yes	3
ENSG00000143627	PKLR	1	155259630	155271225	5313	PKLR	NA	NA	Yes	3
ENSG00000160752	FDPS	1	155278539	155290457	2224	FDPS	NA	NA	Yes	3
ENSG00000160753	RUSC1	1	155290687	155300905	23623	RUSC1	NA	NA	Yes	3
ENSG00000116539	ASH1L	1	155305059	155532598	55870	ASH1L	NA	NA	No	3
ENSG00000125459	MSTO1	1	155579979	155718153	55154	MSTO1	5.68E-14	-	No	3
ENSG00000163374	YY1AP1	1	155629237	155658791	55249	YY1AP1	NA	NA	No	3
ENSG00000132676	DAP3	1	155657751	155708801	7818	DAP3	0.013506	NA	No	3
ENSG00000116580	GON4L	1	155719508	155829191	54856	GON4L	NA	NA	Yes	3
ENSG00000132718	SYT11	1	155829300	155854990	23208	SYT11	NA	NA	Yes	3
ENSG00000143622	RIT1	1	155867599	155881195	6016	RIT1	2.12E-05	NA	Yes	3
ENSG00000132680	KIAA0907	1	155882834	155904191	22889	KIAA0907	NA	NA	No	3
ENSG00000173080	RXFP4	1	155911480	155912625	339403	RXFP4	NA	NA	Yes	3
ENSG00000116584	ARHGEF2	1	155916630	155976861	9181	ARHGEF2	NA	NA	No	3
ENSG00000163479	SSR2	1	155978839	155990750	6746	SSR2	0.00235671	NA	No	3
ENSG00000160803	UBQLN4	1	156005092	156023585	56893	UBQLN4	0.00264926	+	Yes	3
ENSG00000116586	LAMTOR2	1	156024543	156028301	28956	LAMTOR2	NA	NA	Yes	3
ENSG00000132698	RAB25	1	156030951	156040295	57111	RAB25	NA	NA	Yes	3
ENSG00000160785	SLC25A44	1	156163880	156182587	9673	SLC25A44	NA	NA	Yes	3
ENSG00000198715	C1orf85	1	156259880	156265463	112770	C1orf85	NA	NA	Yes	3
ENSG00000189030	VHLL	1	156268415	156269428	391104	VHLL	NA	NA	Yes	3
ENSG00000163467	TSACC	1	156307105	156316786	128229	TSACC	NA	NA	Yes	3
ENSG00000135847	ACBD6	1	180244515	180472089	84320	ACBD6	NA	NA	Yes	4

ENSG00000135835	KIAA1614	1	180882290	180920750	57710	KIAA1614	1.81E-06	-	Yes	4
ENSG00000234237	AL162431.1	1	180941695	180949868	NA	NA	NA	NA	Yes	4
ENSG00000135823	STX6	1	180941861	180992047	10228	STX6	9.71E-09	-	No	4
ENSG00000153029	MR1	1	181003067	181031074	3140	MR1	NA	NA	Yes	4
ENSG00000117280	RAB7L1	1	205737114	205744588	8934	RAB7L1	8.70E-10	NA	No	5
ENSG00000133065	SLC41A1	1	205758221	205782876	254428	SLC41A1	NA	NA	No	5
ENSG00000162877	PM20D1	1	205797150	205819260	148811	PM20D1	NA	NA	Yes	5
ENSG00000198049	AVPR1B	1	206223976	206231639	553	AVPR1B	NA	NA	Yes	5
ENSG00000180667	YOD1	1	207217194	207226325	55432	YOD1	NA	NA	Yes	5
ENSG00000123836	PFKFB2	1	207222801	207254369	5208	PFKFB2	NA	NA	Yes	5
ENSG00000082482	KCNK2	1	215179118	215410436	3776	KCNK2	NA	NA	No	6
ENSG00000268688	AC007382.1	2	37068327	37068530	NA	NA	NA	NA	No	7
ENSG00000115808	STRN	2	37070783	37193615	6801	STRN	NA	NA	No	7
ENSG00000008869	HEATR5B	2	37195526	37311485	54497	HEATR5B	NA	NA	No	7
ENSG00000138083	SIX3	2	45168902	45173216	6496	SIX3	NA	NA	No	8
ENSG00000095002	MSH2	2	47630108	47789450	4436	MSH2	NA	NA	Yes	9
ENSG00000116062	MSH6	2	47922669	48037240	2956	MSH6	0.00489396	NA	No	9
ENSG00000138081	FBXO11	2	48016455	48132932	80204	FBXO11	NA	NA	Yes	9
ENSG00000170802	FOXN2	2	48541776	48606433	3344	FOXN2	5.46E-52	NA	No	9
ENSG00000162869	PPP1R21	2	48667737	48742525	129285	PPP1R21	4.28E-14	NA	Yes	9
ENSG00000177994	C2orf73	2	54557171	54610879	129852	C2orf73	NA	NA	Yes	10
ENSG00000115306	SPTBN1	2	54683422	54896812	6711	SPTBN1	2.51E-07	-	Yes	10
ENSG00000214595	EML6	2	54950636	55199157	400954	EML6	NA	NA	Yes	10
ENSG00000115310	RTN4	2	55199325	55339757	57142	RTN4	NA	NA	Yes	10
ENSG00000085760	MTIF2	2	55463731	55496483	4528	MTIF2	NA	NA	Yes	10
ENSG00000168754	FAM178B	2	97541620	97684175	51252	FAM178B	NA	NA	No	11
ENSG00000144199	FAHD2B	2	97749320	97760619	151313	FAHD2B	NA	NA	No	11

ENSG00000135976	ANKRD36	2	97779233	97930258	375248	ANKRD36	NA	NA	No	11
ENSG00000135940	COX5B	2	98262503	98264846	1329	COX5B	NA	NA	No	11
ENSG00000115073	ACTR1B	2	98272431	98280570	10120	ACTR1B	4.16E-26	+	No	11
ENSG00000115085	ZAP70	2	98330023	98356325	7535	ZAP70	7.74E-43	-	No	11
ENSG00000075568	TMEM131	2	98372799	98612388	23505	TMEM131	NA	NA	No	11
ENSG00000222000	AC092675.3	2	98947852	98972468	NA	NA	NA	NA	Yes	11
ENSG00000144191	CNGA3	2	98962618	99015064	1261	CNGA3	NA	NA	Yes	11
ENSG00000183513	COA5	2	99215773	99224978	493753	COA5	NA	NA	Yes	11
ENSG00000115446	UNC50	2	99225042	99234978	25972	UNC50	NA	NA	Yes	11
ENSG00000071073	MGAT4A	2	99235569	99347589	11320	MGAT4A	NA	NA	Yes	11
ENSG00000158411	MITD1	2	99777890	99797521	129531	MITD1	NA	NA	Yes	11
ENSG00000185414	MRPL30	2	99797542	99814089	51263	MRPL30	NA	NA	Yes	11
ENSG00000115233	PSMD14	2	162164549	162268228	10213	PSMD14	NA	NA	Yes	12
ENSG00000136535	TBR1	2	162272605	162282381	10716	TBR1	NA	NA	Yes	12
ENSG00000144290	SLC4A10	2	162280843	162841792	57282	SLC4A10	NA	NA	No	12
ENSG00000197635	DPP4	2	162848751	162931052	1803	DPP4	NA	NA	No	12
ENSG00000213953	AC018867.1	2	187361840	187365393	NA	NA	NA	NA	Yes	13
ENSG00000268846	AC018867.2	2	187367219	187367356	NA	NA	NA	NA	Yes	13
ENSG00000138448	ITGAV	2	187454792	187545628	3685	ITGAV	NA	NA	Yes	13
ENSG00000144369	FAM171B	2	187558698	187630685	165215	FAM171B	NA	NA	Yes	13
ENSG00000163012	ZSWIM2	2	187692562	187713935	151112	ZSWIM2	0.0346681	NA	Yes	13
ENSG00000064989	CALCRL	2	188207856	188313187	10203	CALCRL	2.84E-05	+	Yes	13
ENSG00000003436	TFPI	2	188328957	188430487	7035	TFPI	NA	NA	No	13
ENSG00000023228	NDUFS1	2	206979541	207024327	4719	NDUFS1	NA	NA	Yes	14
ENSG00000114942	EEF1B2	2	207024309	207027652	619569	EEF1B2	NA	NA	Yes	14
ENSG00000204186	ZDBF2	2	207139387	207179148	57683	ZDBF2	NA	NA	Yes	14
ENSG00000138400	MDH1B	2	207602487	207630271	130752	MDH1B	1.96E-21	NA	Yes	14

ENSG00000118246	FASTKD2	2	207630081	207657233	22868	FASTKD2	NA	NA	Yes	14
ENSG00000118263	KLF7	2	207938861	208031991	8609	KLF7	NA	NA	Yes	14
ENSG00000118260	CREB1	2	208394461	208468155	1385	CREB1	NA	NA	Yes	14
ENSG00000163249	CCNYL1	2	208576264	208626563	151195	CCNYL1	NA	NA	Yes	14
ENSG00000168028	RPSA	3	39448180	39454033	574040	RPSA	1.12E-13	+	No	15
ENSG00000168314	MOBP	3	39508689	39570970	4336	MOBP	NA	NA	No	15
ENSG00000114784	EIF1B	3	40351175	40353915	10289	EIF1B	NA	NA	Yes	15
ENSG00000163638	ADAMTS9	3	64501333	64673676	56999	ADAMTS9	NA	NA	Yes	16
ENSG00000170017	ALCAM	3	105085753	105295744	214	ALCAM	NA	NA	Yes	17
ENSG00000251012	RP11-484M3.5	3	118866222	118906654	NA	NA	NA	NA	No	18
ENSG00000114638	UPK1B	3	118892364	118924000	7348	UPK1B	0.00764953	-	No	18
ENSG00000121578	B4GALT4	3	118930579	118959950	8702	B4GALT4	NA	NA	Yes	18
ENSG00000176142	TMEM39A	3	119148347	119187677	55254	TMEM39A	NA	NA	Yes	18
ENSG00000163389	POGLUT1	3	119187785	119213555	56983	POGLUT1	NA	NA	Yes	18
ENSG00000113845	TIMMDC1	3	119217379	119243937	51300	TIMMDC1	NA	NA	Yes	18
ENSG00000144843	ADPRH	3	119298115	119308792	141	ADPRH	NA	NA	Yes	18
ENSG00000174963	ZIC4	3	147103833	147124647	84107	ZIC4	NA	NA	Yes	19
ENSG00000152977	ZIC1	3	147111209	147228080	7545	ZIC1	NA	NA	Yes	19
ENSG00000144891	AGTR1	3	148415571	148460795	185	AGTR1	NA	NA	Yes	19
ENSG00000153002	CPB1	3	148508889	148577974	1360	CPB1	NA	NA	Yes	19
ENSG00000177565	TBL1XR1	3	176737143	176915261	79718	TBL1XR1	NA	NA	Yes	20
ENSG00000197584	KCNMB2	3	177990720	178562217	10242	KCNMB2	NA	NA	No	20
ENSG00000205835	GMNC	3	190570666	190610218	647309	GMNC	NA	NA	No	21
ENSG00000114315	HES1	3	193853934	193856521	3280	HES1	NA	NA	Yes	22
ENSG00000145217	SLC26A1	4	972861	987228	10861	SLC26A1	3.90E-15	+	No	23
ENSG00000127415	IDUA	4	980785	998316	3425	IDUA	NA	NA	No	23
ENSG00000127418	FGFRL1	4	1003724	1020685	53834	FGFRL1	NA	NA	No	23

ENSG00000109790	KLHL5	4	39046659	39128477	51088	KLHL5	NA	NA	No	24
ENSG00000035928	RFC1	4	39289076	39367995	5981	RFC1	NA	NA	Yes	24
ENSG00000109189	USP46	4	53457138	53525502	64854	USP46	0.00605346	NA	Yes	25
ENSG00000226887	ERVMER34-1	4	53588785	53617807	100288413	ERVMER34-1	NA	NA	No	25
ENSG00000128045	RASL11B	4	53728457	53733000	65997	RASL11B	NA	NA	No	25
ENSG00000184178	SCFD2	4	53739149	54232242	152579	SCFD2	NA	NA	No	25
ENSG00000145358	DDIT4L	4	101107027	101111939	115265	DDIT4L	NA	NA	Yes	26
ENSG00000153064	BANK1	4	102332443	102995969	55024	BANK1	NA	NA	No	26
ENSG00000138821	SLC39A8	4	103172198	103352415	64116	SLC39A8	NA	NA	No	26
ENSG00000138738	PRDM5	4	121606074	121844025	11107	PRDM5	0.00107124	-	No	27
ENSG00000173376	NDNF	4	121956768	121994176	79625	NDNF	NA	NA	Yes	27
ENSG00000035499	DEPDC1B	5	59892739	59996017	55789	DEPDC1B	9.55E-07	+	No	29
ENSG00000164181	ELOVL7	5	60047618	60140216	79993	ELOVL7	NA	NA	No	29
ENSG00000049167	ERCC8	5	60169658	60240900	1161	ERCC8	0.0348806	NA	No	29
ENSG00000153140	CETN3	5	89688078	89705603	1070	CETN3	NA	NA	Yes	30
ENSG00000175745	NR2F1	5	92919043	92930321	7025	NR2F1	NA	NA	Yes	31
ENSG00000185261	KIAA0825	5	93488671	93954309	285600	KIAA0825	NA	NA	Yes	31
ENSG00000133302	ANKRD32	5	93954052	94075141	84250	ANKRD32	NA	NA	Yes	31
ENSG00000168916	ZNF608	5	123972608	124084500	57507	ZNF608	NA	NA	Yes	32
ENSG00000155324	GRAMD3	5	125695824	125832186	65983	GRAMD3	NA	NA	Yes	32
ENSG00000124782	RREB1	6	7107830	7252213	6239	RREB1	0.0210277	-	No	33
ENSG00000203760	CENPW	6	126661320	126670021	387103	CENPW	0.045306	NA	No	35
ENSG00000146374	RSPO3	6	127439749	127518910	84870	RSPO3	NA	NA	Yes	35
ENSG00000016402	IL20RA	6	137321108	137366298	53832	IL20RA	NA	NA	Yes	36
ENSG00000254440	PBOV1	6	138537129	138539627	59351	PBOV1	NA	NA	Yes	36
ENSG00000262543	RP3-422G23.4	6	138699042	138704212	NA	NA	NA	NA	Yes	36
ENSG00000051620	HEBP2	6	138724668	138743334	23593	HEBP2	NA	NA	Yes	36

ENSG00000135540	NHSL1	6	138743180	139013708	57224	NHSL1	NA	NA	No	36
ENSG00000203734	ECT2L	6	139117063	139225207	345930	ECT2L	NA	NA	Yes	36
ENSG00000146386	ABRACL	6	139349819	139364439	58527	ABRACL	NA	NA	Yes	36
ENSG00000112406	HECA	6	139456249	139501939	51696	HECA	NA	NA	Yes	36
ENSG00000164440	TXLNB	6	139561198	139613276	167838	TXLNB	NA	NA	Yes	36
ENSG00000164442	CITED2	6	139693393	139695757	10370	CITED2	NA	NA	Yes	36
ENSG00000071189	SNX13	7	17830385	17980124	23161	SNX13	NA	NA	No	37
ENSG00000048052	HDAC9	7	18126572	19042039	9734	HDAC9	NA	NA	No	38
ENSG00000122691	TWIST1	7	19060614	19157295	7291	TWIST1	NA	NA	Yes	38
ENSG00000106683	LIMK1	7	73497263	73536855	3984	LIMK1	NA	NA	Yes	39
ENSG00000106682	EIF4H	7	73588575	73611431	7458	EIF4H	NA	NA	Yes	39
ENSG00000049541	RFC2	7	73645829	73668774	5982	RFC2	NA	NA	Yes	39
ENSG00000106665	CLIP2	7	73703805	73820273	7461	CLIP2	NA	NA	Yes	39
ENSG00000006704	GTF2IRD1	7	73868120	74016931	9569	GTF2IRD1	NA	NA	Yes	39
ENSG00000077809	GTF2I	7	74071994	74175026	2969	GTF2I	NA	NA	No	39
ENSG00000158517	NCF1	7	74188309	74203659	653361	NCF1	NA	NA	No	39
ENSG00000196275	GTF2IRD2	7	74210483	74267847	84163	GTF2IRD2	6.51E-38	+	No	39
ENSG00000174374	WBSCR16	7	74441226	74490064	653375	WBSCR16	NA	NA	Yes	39
ENSG00000075223	SEMA3C	7	80371854	80551675	10512	SEMA3C	NA	NA	Yes	40
ENSG00000075213	SEMA3A	7	83585093	84122040	10371	SEMA3A	NA	NA	No	41
ENSG00000164815	ORC5	7	103766788	103848495	5001	ORC5	NA	NA	No	42
ENSG00000105851	PIK3CG	7	106505723	106547590	5294	PIK3CG	NA	NA	Yes	43
ENSG00000005249	PRKAR2B	7	106685094	106802256	5577	PRKAR2B	NA	NA	Yes	43
ENSG00000105856	HBP1	7	106809406	106842974	26959	HBP1	NA	NA	Yes	43
ENSG00000164597	COG5	7	106842000	107204959	10466	COG5	0.00739835	NA	No	43
ENSG00000172209	GPR22	7	107110463	107116098	2845	GPR22	NA	NA	No	43
ENSG00000105865	DUS4L	7	107203929	107218906	11062	DUS4L	NA	NA	No	43

ENSG0000075790	BCAP29	7	107220422	107269615	55973	BCAP29	0.00838518	+	Yes	43
ENSG0000091137	SLC26A4	7	107301080	107358254	5172	SLC26A4	NA	NA	No	43
ENSG00000105879	CBLL1	7	107384142	107402112	79872	CBLL1	NA	NA	Yes	43
ENSG0000091140	DLD	7	107531415	107572175	1738	DLD	NA	NA	Yes	43
ENSG00000104756	KCTD9	8	25285366	25315992	54793	KCTD9	NA	NA	Yes	44
ENSG00000184661	CDCA2	8	25316513	25365436	157313	CDCA2	NA	NA	Yes	44
ENSG00000221818	EBF2	8	25699246	25902913	64641	EBF2	NA	NA	Yes	44
ENSG00000221914	PPP2R2A	8	26149007	26230196	5520	PPP2R2A	NA	NA	Yes	44
ENSG00000104765	BNIP3L	8	26240414	26363152	665	BNIP3L	NA	NA	Yes	44
ENSG00000104332	SFRP1	8	41119481	41167016	6422	SFRP1	0.00050797	+	No	45
ENSG00000154188	ANGPT1	8	108261721	108510283	284	ANGPT1	NA	NA	Yes	46
ENSG00000107105	ELAVL2	9	23690102	23826335	1993	ELAVL2	NA	NA	Yes	47
ENSG00000158169	FANCC	9	97861336	98079991	2176	FANCC	7.57E-07	-	Yes	48
ENSG00000185920	PTCH1	9	98205262	98279339	5727	PTCH1	NA	NA	Yes	48
ENSG00000268926	DKFZP434H0512	9	98534605	98537013	NA	NA	NA	NA	Yes	48
ENSG00000182150	ERCC6L2	9	98637983	98776842	101928170	ERCC6L2	NA	NA	Yes	48
ENSG00000130956	HABP4	9	99212483	99253618	22927	HABP4	NA	NA	Yes	48
ENSG00000175029	CTBP2	10	126676421	126849739	1488	CTBP2	NA	NA	No	49
ENSG00000142102	ATHL1	11	289135	296107	80162	ATHL1	1.63E-19	+	No	50
ENSG00000206013	IFITM5	11	298200	299526	387733	IFITM5	NA	NA	No	50
ENSG00000185201	IFITM2	11	307631	315272	10581	IFITM2	3.06E-08	-	No	50
ENSG00000185885	IFITM1	11	313506	315272	8519	IFITM1	NA	NA	No	50
ENSG00000142089	IFITM3	11	319669	327537	10410	IFITM3	1.85E-09	-	No	50
ENSG00000133816	MICAL2	11	12115543	12285334	9645	MICAL2	3.45E-21	-	No	51
ENSG00000133808	MICALCL	11	12297627	12380691	84953	MICALCL	NA	NA	Yes	51
ENSG00000170959	DCDC1	11	30851916	31391357	100506627	DCDC1	NA	NA	Yes	52
ENSG00000170946	DNAJC24	11	31391387	31453396	120526	DNAJC24	NA	NA	Yes	52

ENSG00000148950	IMMP1L	11	31453948	31531192	196294	IMMP1L	NA	NA	Yes	52
ENSG00000109911	ELP4	11	31531297	31805546	26610	ELP4	NA	NA	Yes	52
ENSG00000007372	PAX6	11	31806340	31839509	5080	PAX6	NA	NA	Yes	52
ENSG00000049449	RCN1	11	31833939	32127301	440034	RCN1	NA	NA	Yes	52
ENSG00000184937	WT1	11	32409321	32457176	7490	WT1	NA	NA	Yes	52
ENSG00000165323	FAT3	11	92085262	92629618	120114	FAT3	NA	NA	No	53
ENSG00000166741	NNMT	11	114128509	114184007	101928916	NNMT	NA	NA	No	54
ENSG00000111371	SLC38A1	12	46576846	46663800	81539	SLC38A1	NA	NA	Yes	55
ENSG00000005175	RPAP3	12	48057070	48099844	79657	RPAP3	NA	NA	Yes	55
ENSG00000268069	AC004466.1	12	48178706	48179787	NA	NA	NA	NA	Yes	55
ENSG00000134291	TMEM106C	12	48357352	48362661	79022	TMEM106C	NA	NA	Yes	55
ENSG00000139219	COL2A1	12	48366748	48398269	1280	COL2A1	NA	NA	No	55
ENSG00000257955	RP1-228P16.5	12	48413554	48419165	NA	NA	NA	NA	Yes	55
ENSG00000079387	SENP1	12	48436681	48500091	29843	SENP1	NA	NA	Yes	55
ENSG00000152556	PFKM	12	48498922	48540187	5213	PFKM	1.08E-11	+	Yes	55
ENSG00000177981	ASB8	12	48541571	48574996	140461	ASB8	4.72E-11	NA	Yes	55
ENSG00000177875	C12orf68	12	48577366	48579709	387856	C12orf68	NA	NA	Yes	55
ENSG00000269514	DKFZP779L1853	12	48592170	48595814	NA	NA	NA	NA	Yes	55
ENSG00000172640	OR10AD1	12	48596081	48597170	121275	OR10AD1	NA	NA	Yes	55
ENSG00000177627	C12orf54	12	48876286	48890295	121273	C12orf54	0.00111042	NA	No	55
ENSG00000060709	RIMBP2	12	130880682	131200826	23504	RIMBP2	NA	NA	Yes	56
ENSG00000139746	RBM26	13	79885962	79980612	64062	RBM26	5.69E-06	+	No	57
ENSG00000175198	PCCA	13	100741269	101182686	5095	PCCA	NA	NA	No	59
ENSG00000125266	EFNB2	13	107142079	107187462	1948	EFNB2	NA	NA	Yes	60
ENSG00000134884	ARGLU1	13	107194021	107220512	55082	ARGLU1	NA	NA	Yes	60
ENSG00000100814	CCNB1IP1	14	20779527	20801471	57820	CCNB1IP1	NA	NA	Yes	61
ENSG00000165782	TMEM55B	14	20925878	20929771	90809	TMEM55B	NA	NA	Yes	61



ENSG00000198805	PNP	14	20937113	20945253	4860	PNP	NA	NA	Yes	61
ENSG00000165794	SLC39A2	14	21467414	21470030	29986	SLC39A2	NA	NA	Yes	61
ENSG00000165795	NDRG2	14	21484922	21539031	57447	NDRG2	NA	NA	No	61
ENSG00000255472	RP11-998D10.1	14	21500977	21502054	NA	NA	NA	NA	Yes	61
ENSG00000206150	RNASE13	14	21500979	21502944	440163	RNASE13	NA	NA	Yes	61
ENSG00000165799	RNASE7	14	21510385	21512393	84659	RNASE7	NA	NA	Yes	61
ENSG00000173431	RNASE8	14	21525981	21526614	122665	RNASE8	NA	NA	Yes	61
ENSG00000165801	ARHGEF40	14	21538429	21558399	55701	ARHGEF40	NA	NA	No	61
ENSG00000165804	ZNF219	14	21558205	21572881	51222	ZNF219	NA	NA	Yes	61
ENSG00000232070	TMEM253	14	21567096	21571883	643382	TMEM253	NA	NA	Yes	61
ENSG00000129562	DAD1	14	23033805	23058175	1603	DAD1	NA	NA	Yes	61
ENSG00000196860	TOMM20L	14	58862634	58875419	387990	TOMM20L	NA	NA	Yes	63
ENSG00000165617	DACT1	14	59100685	59115039	51339	DACT1	NA	NA	Yes	63
ENSG00000100592	DAAM1	14	59655364	59838123	23002	DAAM1	NA	NA	Yes	63
ENSG00000126790	L3HYPDH	14	59927081	59951148	112849	L3HYPDH	1.39E-21	-	No	63
ENSG00000139970	RTN1	14	60062694	60337684	6252	RTN1	NA	NA	Yes	63
ENSG00000100664	EIF5	14	103799881	103811362	1983	EIF5	NA	NA	Yes	64
ENSG00000075413	MARK3	14	103851729	103970168	4140	MARK3	NA	NA	Yes	64
ENSG00000166165	CKB	14	103985996	103989448	1152	CKB	NA	NA	Yes	64
ENSG00000166166	TRMT61A	14	103995521	104003410	115708	TRMT61A	8.83E-05	NA	No	64
ENSG00000175779	C15orf53	15	38988799	38992239	400359	C15orf53	NA	NA	Yes	65
ENSG00000137801	THBS1	15	39873280	39891667	7057	THBS1	NA	NA	Yes	65
ENSG00000150667	FSIP1	15	39892232	40075031	161835	FSIP1	NA	NA	No	65
ENSG00000128944	KNSTRN	15	40674922	40686447	90417	KNSTRN	3.03E-38	NA	No	66
ENSG00000128928	IVD	15	40697686	40728146	3712	IVD	NA	NA	Yes	66
ENSG00000128891	C15orf57	15	40820882	40857256	90416	C15orf57	NA	NA	Yes	66
ENSG00000137824	RMDN3	15	41028082	41048049	55177	RMDN3	NA	NA	Yes	66

ENSG00000104142	VPS18	15	41186628	41196173	57617	VPS18	NA	NA	Yes	66
ENSG00000128908	INO80	15	41271078	41408552	54617	INO80	NA	NA	No	66
ENSG00000178997	EXD1	15	41474923	41522941	161829	EXD1	NA	NA	Yes	66
ENSG00000187446	CHP1	15	41523037	41574043	11261	CHP1	NA	NA	Yes	66
ENSG00000104147	OIP5	15	41601466	41624819	11339	OIP5	0.0116217	NA	Yes	66
ENSG00000137804	NUSAP1	15	41624892	41673248	51203	NUSAP1	2.52E-21	+	Yes	66
ENSG00000137806	NDUFAF1	15	41679551	41694717	51103	NDUFAF1	1.75E-24	-	No	66
ENSG00000067221	STOML1	15	74275547	74286963	9399	STOML1	NA	NA	Yes	67
ENSG00000140464	PML	15	74287014	74340153	5371	PML	NA	NA	Yes	67
ENSG00000138629	UBL7	15	74738318	74753523	84993	UBL7	NA	NA	Yes	67
ENSG00000179361	ARID3B	15	74833518	74890472	10620	ARID3B	NA	NA	Yes	67
ENSG00000179335	CLK3	15	74890841	74932057	1198	CLK3	NA	NA	Yes	67
ENSG00000140465	CYP1A1	15	75011883	75017951	1543	CYP1A1	NA	NA	Yes	67
ENSG00000103653	CSK	15	75074398	75095539	1445	CSK	NA	NA	No	67
ENSG00000140506	LMAN1L	15	75105057	75118099	79748	LMAN1L	NA	NA	Yes	67
ENSG00000213578	CPLX3	15	75118888	75124141	594855	CPLX3	NA	NA	Yes	67
ENSG00000140474	ULK3	15	75128457	75135687	25989	ULK3	NA	NA	Yes	67
ENSG00000140497	SCAMP2	15	75136071	75165706	10066	SCAMP2	4.15E-05	+	Yes	67
ENSG00000178802	MPI	15	75182346	75191798	4351	MPI	2.47E-13	+	No	67
ENSG00000178761	FAM219B	15	75192328	75199462	57184	FAM219B	NA	NA	Yes	67
ENSG00000178741	COX5A	15	75212132	75230509	9377	COX5A	NA	NA	Yes	67
ENSG00000178718	RPP25	15	75246757	75249805	54913	RPP25	NA	NA	Yes	67
ENSG00000198794	SCAMP5	15	75249560	75313837	192683	SCAMP5	NA	NA	Yes	67
ENSG00000167173	C15orf39	15	75487984	75504510	56905	C15orf39	NA	NA	Yes	67
ENSG00000169371	SNUPN	15	75890424	75918810	10073	SNUPN	NA	NA	Yes	67
ENSG00000102935	ZNF423	16	49521435	49891830	23090	ZNF423	NA	NA	Yes	68
ENSG00000155393	HEATR3	16	50099852	50140298	55027	HEATR3	NA	NA	Yes	68

ENSG00000141101	NOB1	16	69775770	69788843	28987	NOB1	NA	NA	Yes	69
ENSG00000198373	WWP2	16	69796209	69975644	11060	WWP2	2.53E-10	+	Yes	69
ENSG00000157322	CLEC18A	16	69984810	69998141	348174	CLEC18A	2.23E-29	-	No	69
ENSG00000090857	PDPR	16	70147529	70195203	55066	PDPR	6.30E-06	-	No	69
ENSG00000157335	CLEC18C	16	70207225	70221264	497190	CLEC18C	1.14E-05	+	No	69
ENSG00000269746	AC009060.1	16	70239303	70239683	NA	NA	NA	NA	No	69
ENSG00000269866	FKSG63	16	70258261	70258641	NA	NA	NA	NA	No	69
ENSG00000223496	EXOSC6	16	70284134	70285833	118460	EXOSC6	3.91E-49	-	No	69
ENSG00000090861	AARS	16	70286198	70323446	16	AARS	3.78E-09	+	Yes	69
ENSG00000157349	DDX19B	16	70323566	70369186	11269	DDX19B	NA	NA	Yes	69
ENSG00000260537	RP11-529K1.3	16	70333097	70400163	NA	NA	NA	NA	Yes	69
ENSG00000168872	DDX19A	16	70380732	70407286	55308	DDX19A	NA	NA	No	69
ENSG00000157350	ST3GAL2	16	70413338	70473140	6483	ST3GAL2	NA	NA	No	69
ENSG00000157353	FUK	16	70488324	70514177	197258	FUK	0.0342584	+	No	69
ENSG00000103051	COG4	16	70514471	70557468	25839	COG4	0.00226371	+	Yes	69
ENSG00000189091	SF3B3	16	70557691	70608820	23450	SF3B3	7.67E-12	+	Yes	69
ENSG00000157368	IL34	16	70613798	70694585	146433	IL34	0.00075515	+	No	69
ENSG00000132613	MTSS1L	16	70695107	70719969	92154	MTSS1L	NA	NA	No	69
ENSG00000268927	FLJ00418	16	70695570	70699739	NA	NA	NA	NA	No	69
ENSG00000180917	CMTR2	16	71315292	71323618	55783	CMTR2	0.0123914	NA	No	69
ENSG00000157429	ZNF19	16	71498453	71598992	7567	ZNF19	NA	NA	Yes	69
ENSG00000166747	AP1G1	16	71762913	71843104	164	AP1G1	NA	NA	Yes	69
ENSG00000176692	FOXC2	16	86600857	86602539	2303	FOXC2	NA	NA	Yes	70
ENSG00000176678	FOXL1	16	86609974	86615303	2300	FOXL1	NA	NA	Yes	70
ENSG00000260456	C16orf95	16	87117168	87351022	100506581	C16orf95	NA	NA	No	70
ENSG00000007168	PAFAH1B1	17	2496504	2588909	5048	PAFAH1B1	NA	NA	No	71
ENSG00000108599	AKAP10	17	19807615	19881656	11216	AKAP10	NA	NA	Yes	72

ENSG00000128487	SPECC1	17	19912657	20222339	92521	SPECC1	3.13E-05	NA	No	72
ENSG00000124422	USP22	17	20902910	20947073	23326	USP22	NA	NA	Yes	72
ENSG00000154035	C17orf103	17	21142183	21156722	256302	C17orf103	NA	NA	Yes	72
ENSG00000180329	CCDC43	17	42750437	42767147	124808	CCDC43	NA	NA	Yes	73
ENSG00000108883	EFTUD2	17	42927311	42977030	9343	EFTUD2	NA	NA	Yes	73
ENSG00000167131	CCDC103	17	42976510	42982758	388389	CCDC103	NA	NA	Yes	73
ENSG00000214447	FAM187A	17	42977135	42982758	388389	FAM187A	NA	NA	Yes	73
ENSG00000168517	HEXIM2	17	43238067	43247407	124790	HEXIM2	NA	NA	Yes	73
ENSG00000184922	FMNL1	17	43298811	43324687	752	FMNL1	7.89E-19	+	No	73
ENSG00000159314	ARHGAP27	17	43471275	43511787	201176	ARHGAP27	7.23E-14	-	No	73
ENSG00000225190	PLEKHM1	17	43513266	43568115	9842	PLEKHM1	8.80E-35	+	No	73
ENSG00000185294	SPPL2C	17	43922256	43924438	162540	SPPL2C	5.44E-19	-	No	73
ENSG00000186868	MAPT	17	43971748	44105700	4137	MAPT	NA	NA	Yes	73
ENSG00000256762	STH	17	44076616	44077060	246744	STH	NA	NA	Yes	73
ENSG00000120071	KANSL1	17	44107282	44302733	101929776	KANSL1	1.59E-12	+	No	73
ENSG00000228696	ARL17B	17	44352150	44439130	100506084	ARL17B	2.36E-17	NA	No	73
ENSG00000176681	LRR37A	17	44370099	44415160	474170	LRR37A	4.87E-42	-	No	73
ENSG00000238083	LRR37A2	17	44588877	44633016	474170	LRR37A2	7.91E-44	-	No	73
ENSG00000185829	ARL17A	17	44594068	44657088	100506084	ARL17A	7.42E-31	-	No	73
ENSG00000108379	WNT3	17	44839872	44910520	101929777	WNT3	2.06E-39	-	Yes	73
ENSG00000158955	WNT9B	17	44910567	44964096	7484	WNT9B	NA	NA	Yes	73
ENSG00000198336	MYL4	17	45277812	45301045	4635	MYL4	NA	NA	Yes	73
ENSG00000168646	AXIN2	17	63524681	63557765	8313	AXIN2	NA	NA	Yes	74
ENSG00000154240	CEP112	17	63631656	64188202	201134	CEP112	NA	NA	No	74
ENSG00000091583	APOH	17	64208151	64252643	350	APOH	NA	NA	No	74
ENSG00000154229	PRKCA	17	64298754	64806861	5578	PRKCA	NA	NA	Yes	74
ENSG00000158270	COLEC12	18	319361	500722	81035	COLEC12	NA	NA	Yes	75

ENSG00000197360	ZNF98	19	22573821	22715287	148198	ZNF98	NA	NA	Yes	76
ENSG00000196172	ZNF681	19	23921997	23941693	148213	ZNF681	7.69E-14	+	No	76
ENSG00000205246	RPSAP58	19	23945807	24010937	NA	RPSAP58	NA	NA	No	76
ENSG00000213967	ZNF726	19	24097678	24127961	730087	ZNF726	NA	NA	Yes	76
ENSG00000125740	FOSB	19	45971253	45978437	2354	FOSB	NA	NA	Yes	77
ENSG00000125741	OPA3	19	46030685	46105470	80207	OPA3	NA	NA	No	77
ENSG00000177464	GPR4	19	46093022	46105466	2828	GPR4	NA	NA	No	77
ENSG00000125746	EML2	19	46110252	46148887	24139	EML2	NA	NA	Yes	77
ENSG00000267757	C19orf83	19	46144752	46146098	100287177	C19orf83	NA	NA	Yes	77
ENSG00000125743	SNRPD2	19	46190712	46195827	6633	SNRPD2	NA	NA	Yes	77
ENSG00000011478	QPCTL	19	46195741	46207247	54814	QPCTL	NA	NA	Yes	77
ENSG00000177051	FBXO46	19	46213887	46234162	23403	FBXO46	NA	NA	Yes	77
ENSG00000237452	AC074212.3	19	46236509	46267792	NA	NA	NA	NA	Yes	77
ENSG00000171940	ZNF217	20	52183604	52226446	7764	ZNF217	NA	NA	Yes	78
ENSG00000189060	H1FO	22	38201114	38203442	3005	H1FO	NA	NA	Yes	79
ENSG00000100116	GCAT	22	38203912	38213183	23464	GCAT	NA	NA	Yes	79
ENSG00000100124	ANKRD54	22	38226862	38245334	129138	ANKRD54	NA	NA	Yes	79
ENSG00000100129	EIF3L	22	38244875	38285414	51386	EIF3L	NA	NA	Yes	79
ENSG00000100139	MICALL1	22	38301664	38338829	85377	MICALL1	NA	NA	No	79
ENSG00000100142	POLR2F	22	38348614	38437922	5435	POLR2F	NA	NA	No	79
ENSG00000100151	PICK1	22	38452318	38471708	9463	PICK1	1.67E-18	NA	Yes	79
ENSG00000100156	SLC16A8	22	38474141	38480100	23539	SLC16A8	NA	NA	Yes	79
ENSG00000128298	BAIAP2L2	22	38480896	38506677	80115	BAIAP2L2	NA	NA	No	79
ENSG00000184381	PLA2G6	22	38507502	38601697	8398	PLA2G6	0.0113973	NA	Yes	79
ENSG00000185022	MAFF	22	38597889	38612518	23764	MAFF	NA	NA	Yes	79
ENSG00000198792	TMEM184B	22	38615298	38669040	25829	TMEM184B	NA	NA	Yes	79
ENSG00000213923	CSNK1E	22	38686697	38794527	1454	CSNK1E	NA	NA	Yes	79

ENSG00000100201	DDX17	22	38879445	38903665	10521	DDX17	NA	NA	Yes	79
ENSG00000100206	DMC1	22	38914954	38966291	11144	DMC1	NA	NA	Yes	79
ENSG00000100226	GTPBP1	22	39101728	39134304	9567	GTPBP1	NA	NA	Yes	79
ENSG00000221890	NPTXR	22	39214457	39239987	23467	NPTXR	NA	NA	Yes	79
ENSG00000244509	APOBEC3C	22	39410088	39416357	27350	APOBEC3C	NA	NA	Yes	79
ENSG00000100321	SYNGR1	22	39745930	39781593	9145	SYNGR1	NA	NA	Yes	79
ENSG00000100324	TAB1	22	39795746	39833065	10454	TAB1	NA	NA	Yes	79
ENSG00000100335	MIEF1	22	39895437	39914137	54471	MIEF1	NA	NA	Yes	79
ENSG00000186732	MPPED1	22	43807202	43903728	758	MPPED1	6.39E-06	-	No	80